Delft University of Technology

Assessing the Performance of the Geertsma Model for Surface Uplift Across Multiple CCS Sites

Author:
Songbai Zhou (5672767)

Project duration: August, 2024 – ,May 2025
Thesis committee:
Prof.dr.ir.Femke Vossepoel, Graduation Chair
Prof.dr.Sebastian Geiger, Secondary Supervisor
Gabriel Serrao Seabra, Msc, Assessor

Abstract

In the context of addressing climate change and achieving carbon neutrality, carbon dioxide capture and storage (CCS) technology is widely used to reduce greenhouse gas emissions. However, the surface uplift caused by CO_2 injection still lacks systematic theoretical understanding and quantitative prediction methods, especially in the early stages of the project, which is limited by complex geological conditions and insufficient data. As an analytical solution method, the Geertsma model provides a possibility for the preliminary evaluation of CCS surface deformation with its high efficiency and simplicity.

Based on the Geertsma analytical model, this study established a multi-site surface uplift prediction framework, selected five representative CCS projects, In Salah, Sleipner, Weyburn, Gundih and Saskatchewan, as research objects, collected their field geological parameters, applied full factorial design to evaluate the sensitivity of the model input parameters to the prediction results, and compared and verified them with the CMG-GEM numerical simulation results. The results show that the Geertsma model can reasonably reflect the impact of pressure changes on surface deformation under the assumption of a uniform elastic medium and a disc-shaped reservoir. Sensitivity analysis further revealed that reservoir thickness, pressure change, and reservoir depth are the key factors affecting the amplitude of surface uplift. While the influence of Poisson's ratio is relatively small.

Through multi-site analysis and model comparison, this study verified the applicability and limitations of the Geertsma model in early site selection assessment and parameter sensitivity analysis of CCS. It provided a theoretical basis and technical reference for improving the safety and prediction ability of CO_2 geological storage projects.

Contents

Nomenclature

Abbreviations

Abbreviation	Definition
CO_2	Carbon Dioxide
CCS	Carbon Capture and Storage
CMG	Computer Modelling Group
GEM	General Equation of State Simulator
THMC	Thermal, Hydraulic, Mechanical, and Chemical
InSAR	Interferometric Synthetic Aperture Radar
DOE	Design of Experiments
AUC	Area Under the Curve
ANOVA	Analysis of Variance
FFD	Full Factorial Design
DF	Degrees of Freedom
SS	Sum of Squares
MS	Mean Square
EOR	Enhanced Oil Recovery
FLAC3D	Fast Lagrangian Analysis of Continua in 3 Dimensions

Symbols

Symbol	Definition
R_0	Initial radius of the reservoir
R	Reservoir radius
D	Depth to the center of the reservoir
H	Thickness of the reservoir layer
ν	Poisson's ratio
E	Young's modulus
Δp	Pressure change in the reservoir
C_m	Uniaxial compaction coefficient
σ	Stress
ε	Strain
F	Force
A	Cross-sectional area
Δh	Vertical deformation (change in height)
h	Original thickness
P_f	Pore fluid pressure
σ'	Effective stress
α	Biot coefficient
u_z	Vertical displacement at the surface
r	Radial distance from injection point
J_0, J_1	Bessel functions of the first kind (orders 0 and 1)
V	Volume of the strain nucleus / disk

List of Figures

List of Tables

1 Introduction

1.1 Background

In today's industrialized societies, rapid economic development has led to the extensive exploitation of fossil fuels. This, in turn, has caused a significant increase in carbon dioxide (CO_2) emissions, which impact the natural ecosystems that humans rely on for survival (Pradhan, Nair, Hall, & Bennett, 2024). From 1900 to 2023, energy-related CO_2 emissions have increased by a total of 37.2 gigatonnes (International Energy Agency, 2023). Carbon dioxide is recognized as one of the primary greenhouse gases (Aminu, Nabavi, Rochelle, & Manovic, 2017), and the increase in CO_2 emissions has resulted in various global climate issues, such as global warming and rising sea levels (Falkowski et al., 2000). In the foreseeable future, fossil fuels will continue to be a key component of the global energy mix. Carbon capture and storage (CCS) represents the most direct and essential technological approach to reduce CO_2 emissions and achieve low carbon utilization of fossil energy (Abidoye, Khudaida, & Das, 2015). CCS plays a significant role in supporting the goal of carbon neutrality.

Geological storage of CO_2 involves injecting captured carbon dioxide into deep geological formations and isolating it from the atmosphere for extended periods. As illustrated in Figure 1.1, suitable storage sites are typically found at depths of 800 to 1,000 meters, in reservoirs with good permeability, and sealed by low-permeability cap rocks. The primary types of reservoirs used for this purpose include saline aquifers, oil and gas fields, and coal seams. Among these, deep saline aquifers represent approximately 98% of the overall storage capacity due to their widespread availability (Enyi et al., 2023). Oil and gas fields are also excellent candidates for CO_2 storage, as they possess comprehensive geological exploration data and well-developed surface infrastructure. Additionally, injecting CO_2 into these fields can enhance oil recovery.

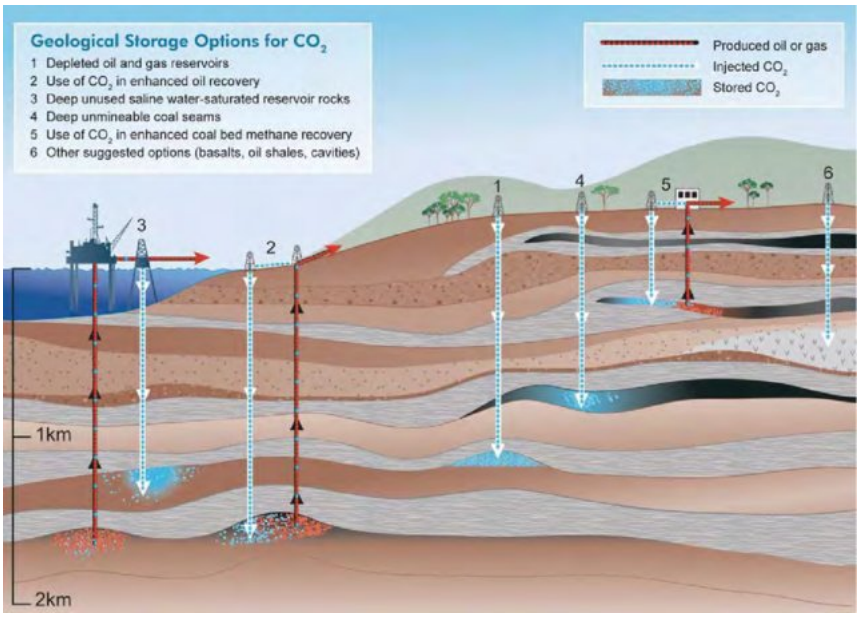

Figure 1.1: Options for the geological storage of CO_2

Source: (Metz et al., 2005)

The process of CO_2 storage in reservoir rocks is complex, influenced by factors such as reservoir properties and geochemical reactions, and involves coupled interactions among thermal, hydraulic, mechanical, and chemical fields (T-H-M-C) (Yin, Dusseault, & Rothenburg, 2011). CO_2 injection leads to significant fluid pressure buildup, causing changes in the effective stress field, affecting rock porosity, permeability, and capillary pressure, thereby influencing CO_2 injection and flow. The injected CO_2 is in a supercritical state, with a temperature significantly lower than the surrounding formation, leading to local temperature variations that alter CO_2 fluid properties such as density, viscosity, and solubility. These changes affect its flow characteristics, and thermal stresses resulting from temperature differences directly alter the stress state of the rock (Xiao, 2016). CO_2 readily dissolves in water, reacting with surrounding rock minerals, potentially dissolving the rock or precipitating as calcium carbonate, and interacting with organic matter in the caprock, altering its permeability and porosity. In addition, the chemical reaction rate of CO_2 in porous media is influenced by factors such as temperature, pressure, seepage velocity, and the diffusion rate of CO_2 (Song & Zhang, 2013).

The primary mechanisms of CO_2 geological storage include (1) structural trapping, where low-permeability caprocks prevent CO_2 migration; (2) capillary trapping, where CO_2 is immobilized by capillary forces in pore structures; (3) adsorption trap-

ping, where CO_2 adsorbs onto clay mineral surfaces; (4) dissolution trapping, where CO_2 dissolves in formation water or oil; and (5) mineral trapping, where CO_2 reacts with rock to form carbonate minerals. After CO_2 is injected into the formation, it is initially trapped in oil and gas reservoirs or deep saline aquifers. The movement of CO_2 is governed by multiphase flow processes, primarily driven by injection pressure and buoyancy caused by density differences (Class et al., 2009). Over time, the free-phase CO_2 migrates slowly upward through rock permeability pathways, and the remaining CO_2 becomes trapped in pores, dissolved in formation water, or precipitated as carbonate minerals (Jiang, 2011).

Geological storage of CO_2 carries inherent risks. If CO_2 migrates vertically to near-surface areas, it may pose risks like shallow groundwater contamination and atmospheric leakage. Therefore, before CO_2 injection operations, it is essential to conduct mechanical analyses and stability assessments of the reservoir-caprock system. Caprock typically consists of undisturbed, low-permeability, thick, and laterally extensive strata, commonly composed of shale, mudstone, and carbonate rocks. These formations possess high capillary entry pressures and breakthrough pressures, which help prevent the leakage of injected fluids. During CO_2 storage, the caprock must withstand both the short-term excess injection pressure and the long-term buoyancy-driven pressure (Espinoza & Santamarina, 2017). Figure 1.2 illustrates the geomechanical issues in CCS (Carbon Capture and Storage) projects.

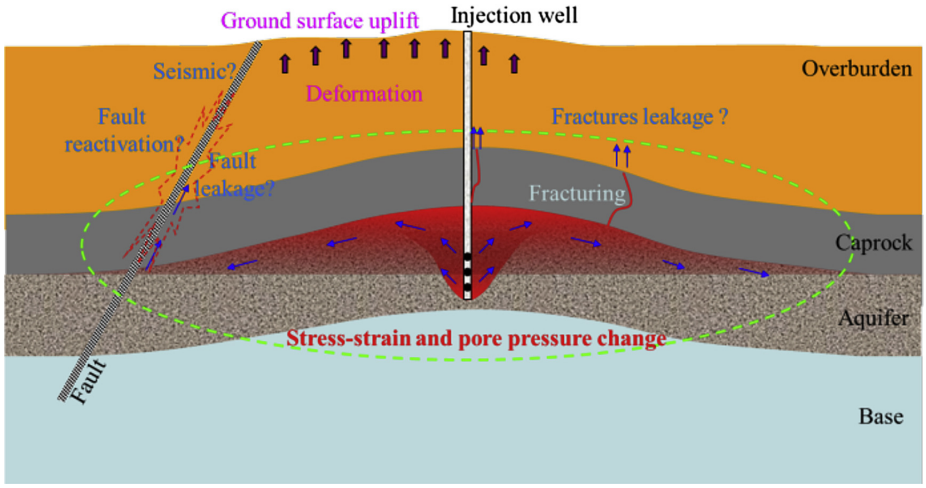

Figure 1.2: Geomechanical issues induced by CO_2 injection, migration and storage

Source: (Li, 2016)

According to Figure 1.2, the CO_2 injection process leads to geomechanical problems. CO_2 is injected mainly into the deep aquifer and gradually accumulates at the bottom of the caprock, leading to a significant increase in pore pressure. This increase in pressure causes an upward deformation of the cap rock, affecting its integrity. If there are natural cracks or faults in the cap rock, the increase in pressure may lead to the crack's extension or the fault's reactivation, increasing the risk of CO_2 leakage. In addition, CO_2 flow and pressure changes can cause stress-strain changes in the reservoir and its overburden, leading to rock rupture, fault leakage, or even seismic activity (Li, 2016).

According to the tracking data of the Global CCS Institute, there are currently 41 CCS projects in operation, and 351 projects are in the development stage. In addition, new CCS projects are announced almost every week. In this rapidly developing context, the study of geomechanical problems has become particularly important because it is directly related to the safety and sustainability of CCS projects.

1.2 Overview of Selected CCS Sites

Five different CCS sites were considered in this study to evaluate the surface uplift caused by CO_2 injection at these sites. Each site has different geological conditions and CO_2 injection schemes. The geographic distribution of the five locations is shown in Figure 1.3. Among the five locations, three significant CCS projects that have stored millions of tons of carbon dioxide are located in In Salah, Weyburn, and Sleipner. Because surface uplift has been observed through site monitoring, the In Salah site is frequently used in surface uplift research. In contrast, Sleipner has not seen any overt surface uplift, and the Weyburn area has not seen any overt surface uplift but has seen numerous microseismic phenomena (J. P. Verdon et al., 2013). The three sites were chosen as research objects in this study primarily because of their distinct geological characteristics.

Gundih and Saskatchewan are two minor CCS projects. The project is still in its early phases at these two locations. In

addition to augmenting the variations in surface displacement between CCS projects of varying sizes, selecting these two projects might offer some recommendations for the project from the beginning.

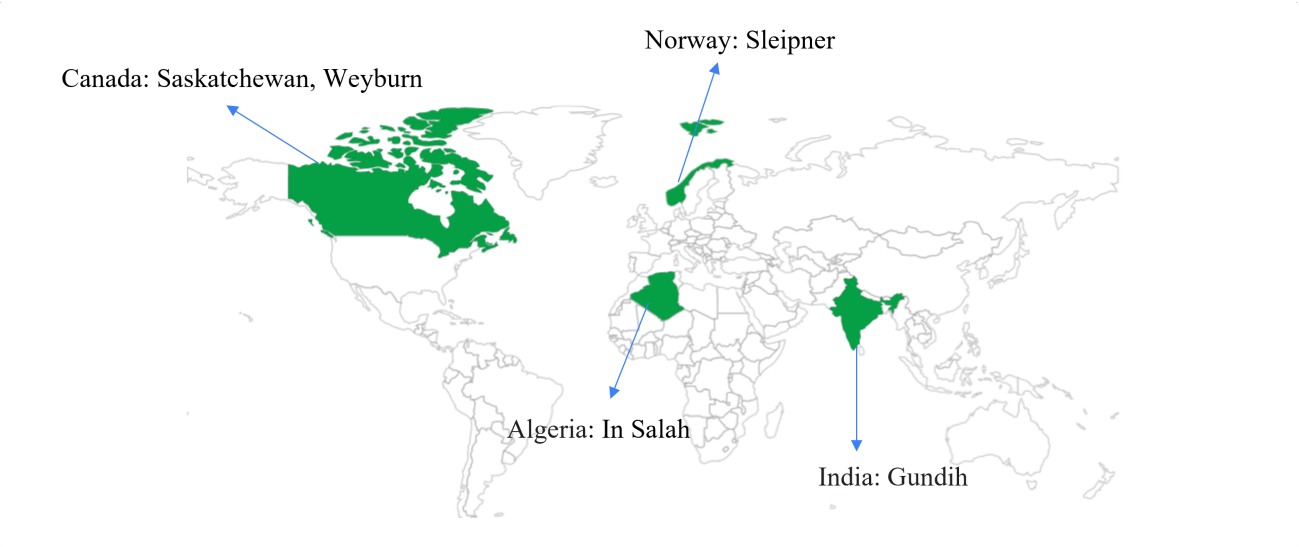

Figure 1.3: Geographical Distribution of Selected CCS Sites

1.2.1 In Salah Field

The In Salah CO_2 storage project in Algeria is one of the most extensively studied sites in terms of surface displacement monitoring. Satellite-based INSAR analysis revealed a surface uplift of approximately 20 mm over three years near the KB503 well, with additional uplift observed near other injection wells (Figure 1.4).

Initiated in 2004, this project was the first in the world to inject CO_2 into a deep natural gas reservoir on a commercial scale. It is estimated that 1.7×10 t of CO_2 will eventually be stored in sandstone layers at depths of 1800–1900 m (J. Rutqvist, Vasco, & Myer, 2010; Rutqvist & Tsang, 2002; Preisig & Prévost, 2011). The geological structure of the area is stable: the reservoir sandstone has low permeability, and the overlying 900 m thick caprock provides sufficient sealing capacity for safe storage.

As one of the earliest sites with long-term satellite-based displacement monitoring, In Salah has become a benchmark for evaluating uplift due to CO_2 injection. Therefore, many researchers have applied numerical simulation to study the mechanical response of the reservoir and surrounding strata.

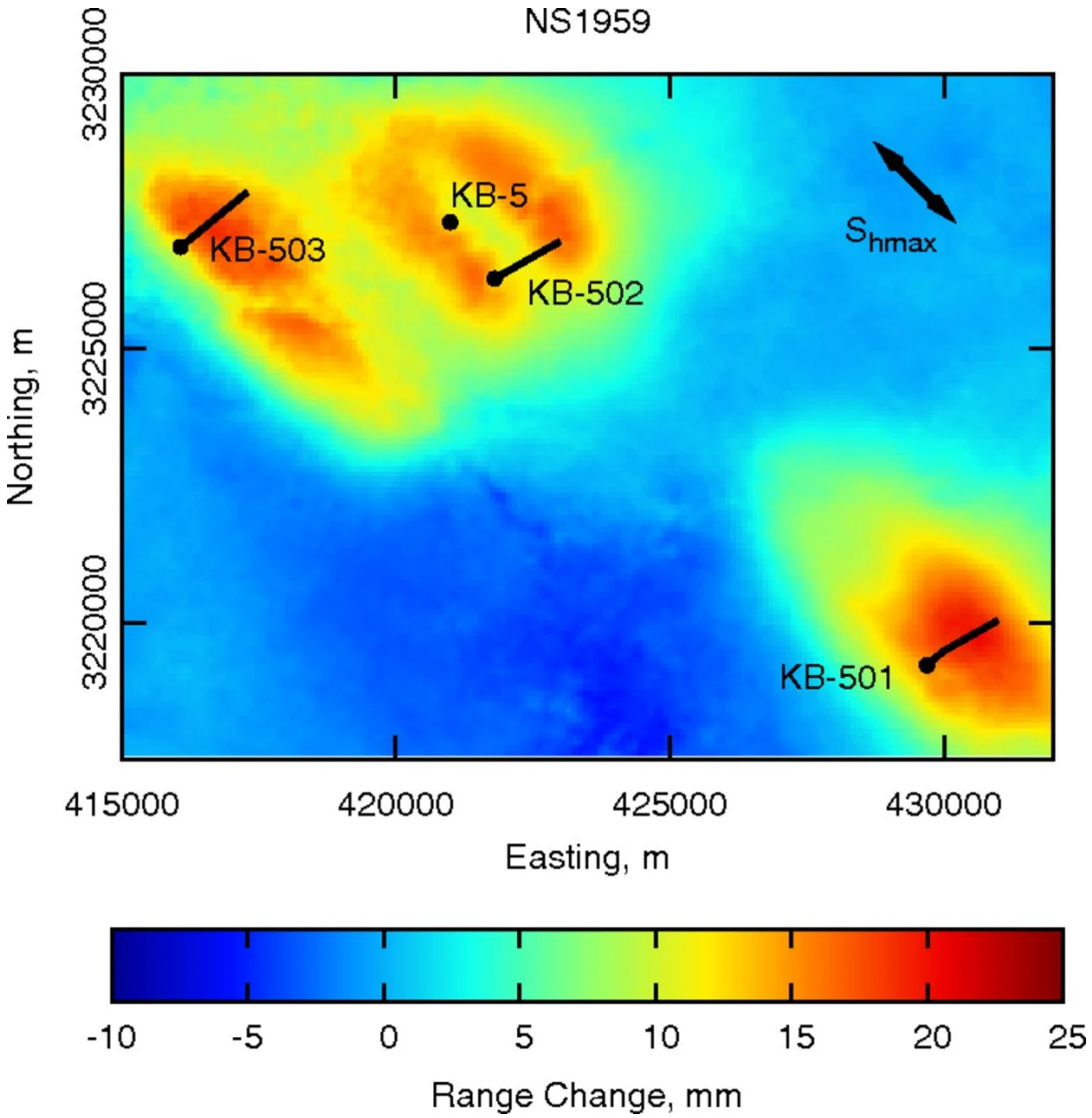

Figure 1.4: InSAR measured surface deformations as of March 2010.

Source: (White et al., 2014)

1.2.2 Sleipner Field

The Sleipner site is located in a saline aquifer in the Norwegian North Sea and is the world's first large-scale CO_2 geological storage project. Since its launch in 1996, the Sleipner project has injected about 1 million tons of CO_2 annually and is still ongoing. One important layer for storing CO_2 in the region is the Utsira sandstone layer. About 900 to 1500 meters deep, it is a typical multi-layer sandstone structure. The high porosity and permeability of the Utsira sandstone make it an ideal material for CO_2 storage and migration (Zweigel, Arts, Lothe, & Lindeberg, 2004).

Despite these advantageous circumstances, the geomechanical impact of CO_2 injection at Sleipner is minimal because the pressure changes in the reservoir brought on by injection are minimal. Monitoring has not placed much emphasis on surface deformation because it is minimal. Rather, the location has been thoroughly investigated using wellhead pressure measurements and time-lapse seismic surveys (J. P. Verdon et al., 2013). A comparatively low geological risk is indicated by the lack of stress concentration zones and the low level of microseismic activity.

1.2.3 Weyburn Field

The Weyburn oil field is in the Wilston sedimentary basin in Saskatchewan, Canada. Since 2000, the Weyburn project has injected about 16 million tons of CO_2. The oil field reservoir consists of two main parts: the upper Marly unit and the lower Vuggy unit (Figure 1.5). With the injection of CO_2, the change in pore pressure triggers stress redistribution in the reservoir, especially in the stress adjustment process of the cap layer M03F and Watrous layer, which may lead to microseismic activity.

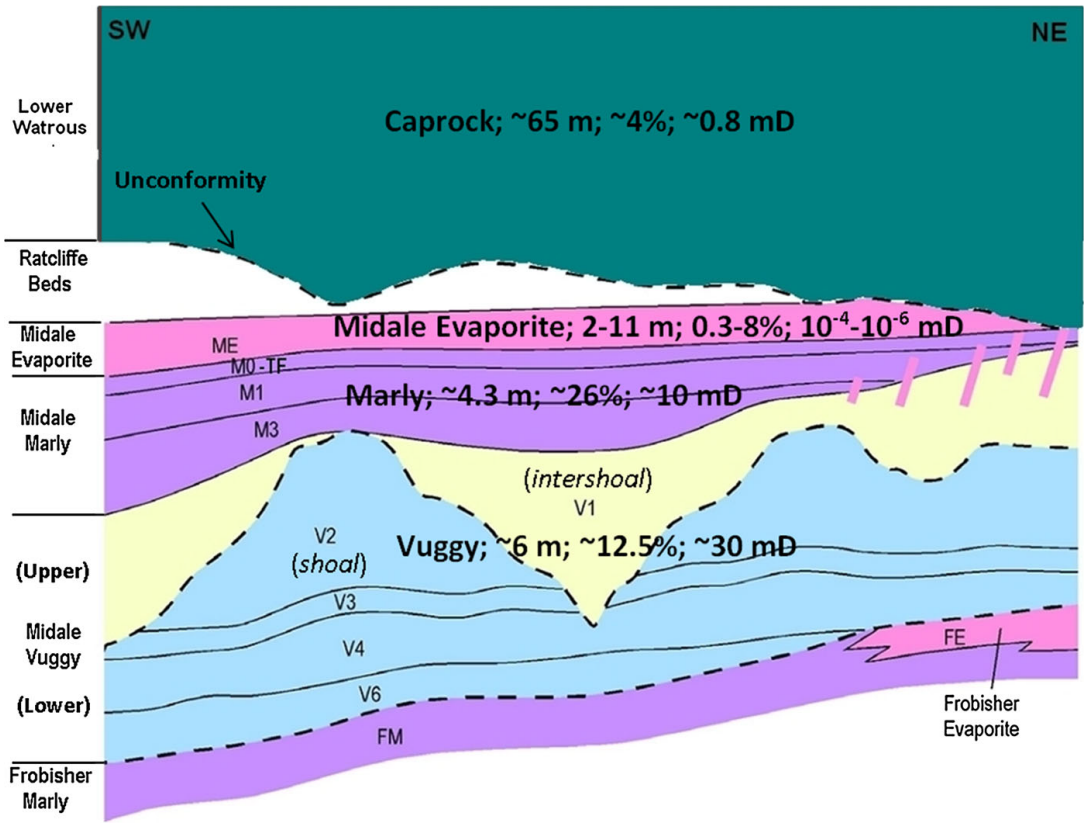

Figure 1.5: Conceptual generalized cross-section of the Weyburn reservoir and its seal layers

Source: (Khazaei & Chalaturnyk, 2017)

The geomechanical research on the Weyburn area is mainly carried out through GEM and FLAC3D models, which combine one-dimensional and three-dimensional coupling analysis to study the impact of reservoir pore pressure changes on surface deformation and stress distribution (Khazaei & Chalaturnyk, 2017). The GEM model is used for historical matching of reservoir pore pressure, and the FLAC3D model is used to analyze the geomechanical response of the cap layer. Although these simulation results provide an important basis for understanding the geological risks in CCS projects, their calculation process requires a lot of time and resources (J. P. Verdon et al., 2013).

1.2.4 Gundih Field

The Gundih CCS project is the first CCS pilot project in Indonesia. The project will be built on Java's earthquake-prone island, making the project more challenging, so safety issues must be prioritized first. The project plans to inject carbon dioxide into the Ngrayong Formation, which is composed of silty sandstone at a depth of about 800m. The project plans to inject about 30 tons of carbon dioxide daily, or 20,000 tons of carbon dioxide over two years (Sule, Kadir, Hato, Matsuoka, & Prabowo, n.d.). A study calculated the surface deformation results in the area through a coupled model (Figure 1.6), and the results showed that the predicted surface uplift was less than 0.2 mm (Suhendi, Sahara, & Sule, 2019).

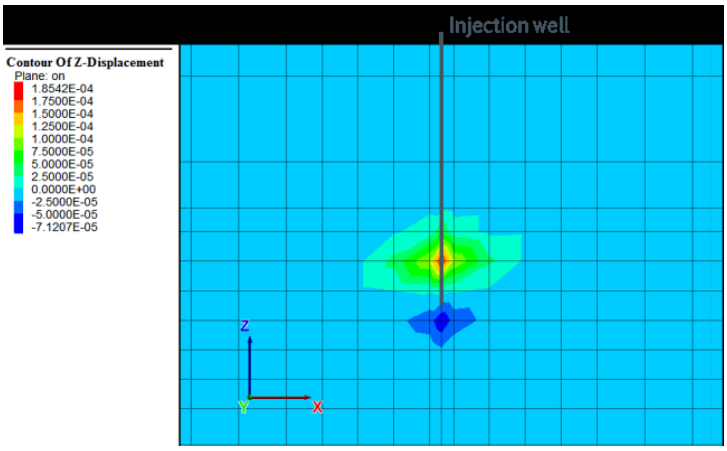

Figure 1.6: Vertical displacement around injection point after 27 days injection in Gundih

Source: (Suhendi et al., 2019)

1.2.5 Saskatchewan Field

The Saskatchewan CCS project is located in southeastern Saskatchewan, Canada. It started in 2012 and is a collaborative project integrating CO_2 storage research, monitoring, and verification. The project serves as a buffer storage project for Boundary Dam, the world's first commercial post-combustion CO_2 capture power plant. Saskatchewan's reservoir consists of brine-filled clastic rock formations, mainly the Deadwood and Winnipeg formations, with a burial depth of between 3150 and 3350 meters. These formations have good conditions for CO_2 injection and long-term storage because they are topped by impermeable sealing layers that effectively prevent the upward migration of CO_2.

The main goal of the project is to ensure safe and long-term CO_2 storage, supported by integrated monitoring technologies to track underground fluid movement, pore pressure evolution, and potential surface deformation. During CO_2 injection, vertical deformation is accurately monitored by InSAR, providing high temporal and spatial resolution. This allows researchers to detect natural and anthropogenic ground movements before and after CO_2 injection. In addition to monitoring, studies have also simulated the deformation expected to be caused by CO_2 injection. Figure 1.7 shows that the maximum vertical deformation near the injection well can reach 1.6 cm per year (Samsonov, Czarnogorska, & White, 2015).

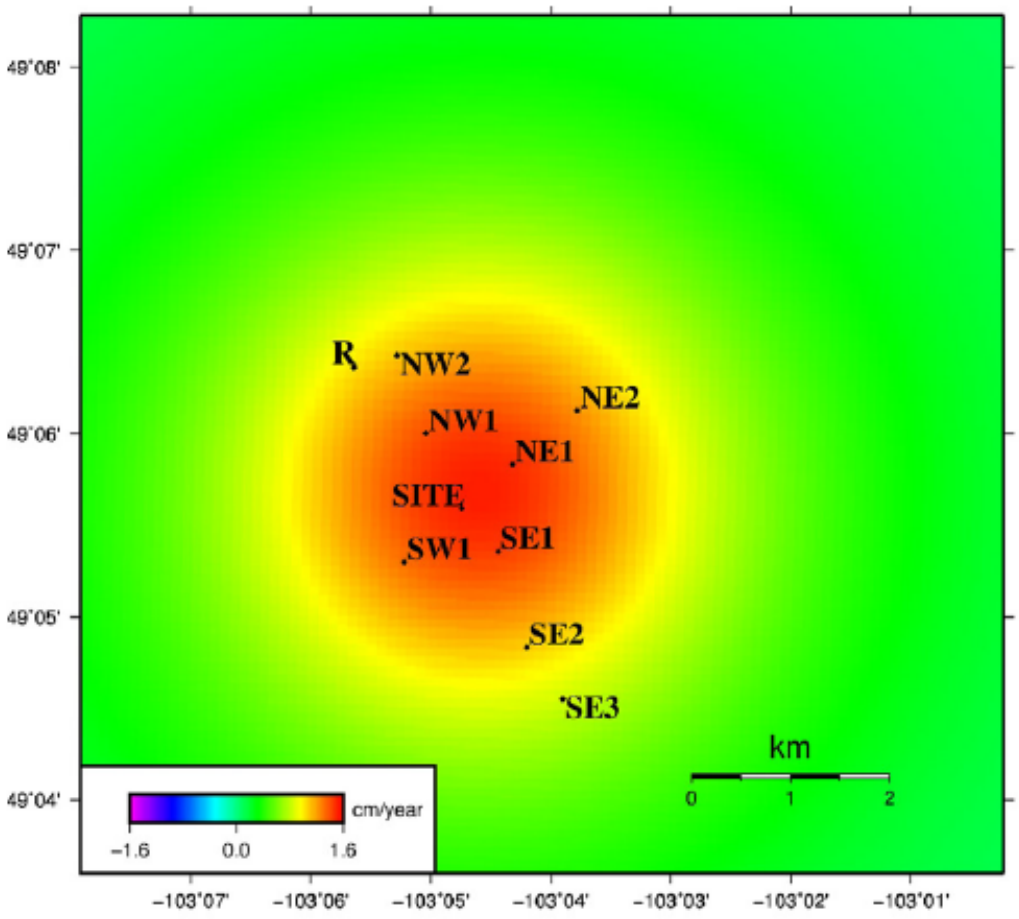

Figure 1.7: Modeled vertical deformation rates computed for elastic point source due to injection of 1500 tonne/day of CO_2 at depth of 3250 m

Source: (Mogi, 1958; Samsonov et al., 2015)

1.3 Research Objectives

The massive emission of greenhouse gases, such as carbon dioxide, has led to global warming (Jeffry et al., 2021). To mitigate this, CCS projects have been widely implemented over the past few decades (Budinis, Krevor, Mac Dowell, Brandon, & Hawkes, 2018). However, the surface uplift resulting from CO_2 injection remains poorly understood (Teatini, Gambolati, Ferronato, Settari, & Walters, 2011). Pressure build-up in the reservoir during injection can deform both the reservoir and the overburden, potentially leading to caprock fracturing and CO_2 leakage (Class et al., 2009).

The Geertsma model provides a simplified yet effective approach for estimating surface deformation due to pressure changes in the reservoir. In contrast, satellite and leveling methods used to monitor uplift are constrained by spatial coverage and accuracy (Zhang, Hao, Yu, Li, & Xu, 2018). Numerical simulations, while powerful, require complex models and substantial computational resources, making them difficult to apply in the early stages of CCS projects (Jun, Song, Wang, & Weijermars, 2023).

Therefore, this study aims to apply the Geertsma model to compute surface uplift across five CCS sites, using site-specific geological parameters. A full factorial experimental design is implemented to explore the sensitivity of uplift predictions to model inputs and to assess the model's performance in practical scenarios. The following research questions are addressed in this work:

- To what extent can the Geertsma model quantitatively predict surface uplift in CCS applications?
- How sensitive is the predicted surface uplift to changes in key model parameters, and which parameters have the most or least influence?
- How do geological conditions and site-specific parameters influence the accuracy and applicability of the Geertsma model across different CCS sites?

1.4 Report Structure

This report is divided into six chapters. Chapter 1 introduces the research background of CCS technology, outlines the geomechanical problems caused by CO_2 injection, and clarifies the main objectives of this study. Chapter 2 describes the physical mechanism of surface uplift, the theoretical basis of the Geertsma model and its mathematical expression, and explains the application of full-factor experiments in CCS sensitivity analysis. The techniques employed in this study, including data collection, factorial design, and CMG, are covered in Chapter 3. Chapter 4 presents the sensitivity analysis results and quantifies each parameter's influence on the maximum surface uplift value and the uplift distribution area. Chapter 5 compares and analyzes the surface uplift results of the Geertsma model and those in the literature using five typical CCS projects as cases, and evaluates the applicability and accuracy of the model under different geological conditions. Finally, Chapter 6 summarizes the research work, summarizes the main findings, points out the limitations of the Geertsma model in CCS applications, and proposes possible directions for future research.

2 Measurements and Models of Uplift

It is well known that the extraction of fluids such as groundwater, gas, and oil can cause land subsidence. The magnitude, timing, and area of land subsidence depend on many factors, including the amount of fluid extracted, the drop in pore pressure, the depth, volume, and permeability of the formation from which it was extracted, and the geomechanical properties of the reservoir. However, surface uplift caused by subsurface fluid injection has received little attention and recognition, even though such projects have existed for over half a century (Teatini et al., 2011).

In most cases, fluid injection projects occur in sparsely populated areas, and measuring surface displacement is not a priority. The high cost of measuring surface displacement is also one of the reasons why surface displacement in injection projects is not given much attention. Some projects cause small surface displacements that do not cause harm, so no reports exist. However, with the large increase in CCS projects, some projects are located near towns and villages, so it is important to study surface displacement in CCS projects. In the past decade, InSAR has increased rapidly, helping researchers explore uplift areas. In recent years, ground and borehole inclinometers have been widely used to monitor ground uplift in relatively small areas (Galloway & Hoffmann, 2007).

There are two types of modeling approaches for surface uplift: analytical solutions and numerical solutions. In general, surface uplift is driven by increased pore pressure in the formation, and a computational method that combines the geomechanical response and formation characteristics with a numerical reservoir fluid flow model is the numerical solution. However, the solution requires fairly sophisticated modeling, including the non-homogeneous surroundings of the reservoir, detailed production, and injection data. Such detailed subsurface data are often lacking in the early stages of a project. The need for computational power and cumbersome upgrades to numerical simulation software make this method costly and time-consuming (J. Rutqvist, Wu, Tsang, & Bodvarsson, 2002; J. Rutqvist et al., 2010).

Against this background, fast and easy-to-use analytical solution methods are of interest. Geertsma presents an analytical model for estimating the subsidence in a confined cylindrical space at a specific formation (pressure decay) based on a Bessel function integral assuming a uniform pressure drop in a bounded reservoir space. The model uses the nucleus of strain concept (Mindlin & Cheng, 1950a) to solve for displacement in the production formation (Weijermars, 2023). The solution is based on the strain kernel approach and utilizes the similarities between the theory of thermoelasticity and the theory of poroelasticity. Such analytical solutions have a wide range of applications in the petroleum industry for estimating land displacement and reservoir compaction (Park, Bjørnarå, & Bohloli, 2021; Park, Eiken, Bjørnarå, & Bohloli, 2021).

The advantages of the Geertsma model are its simplicity and efficiency. Unlike numerical methods such as finite element analysis, the closed-form solution provided by the Geertsma equation is computationally inexpensive but robust. This makes it well suited for:

1. **Efficient uplift modeling**: estimating uplift due to fluid injection.
2. **Sensitivity analysis**: understanding how reservoir geometry and rock properties affect predicted uplift.

The derivation of the Geertsma model is based on the following assumptions (Geertsma, 1973):

1. The underground medium is continuous, uniform, and has the same elastic properties in all directions.
2. The medium behaves as purely elastic, which means deformation is recoverable.
3. The reservoir is infinitely extended in the lateral direction to simplify the boundary conditions (neglect the lateral strain).
4. The total vertical stress acting on the reservoir remains constant.

These assumptions enable the Geertsma model to derive a closed-form analytical solution with high computational efficiency when calculating surface displacements. Of course, these assumptions also limit the model's applicability, so exploring its applicability with sensitivity analysis is necessary (Mehrabian & Abousleiman, 2015).

2.1 Physical Mechanism of Uplift in Disk-Shaped Reservoirs

The key results of the Geertsma equation include vertical displacement (i.e., subsidence or uplift above the reservoir), radial displacement (lateral deformation), and stress changes. The focus of this study is the surface uplift above the reservoir. The Geertsma equation is for disk-shaped reservoirs, while the nucleus of strain considers compaction caused by a sphere at the center.

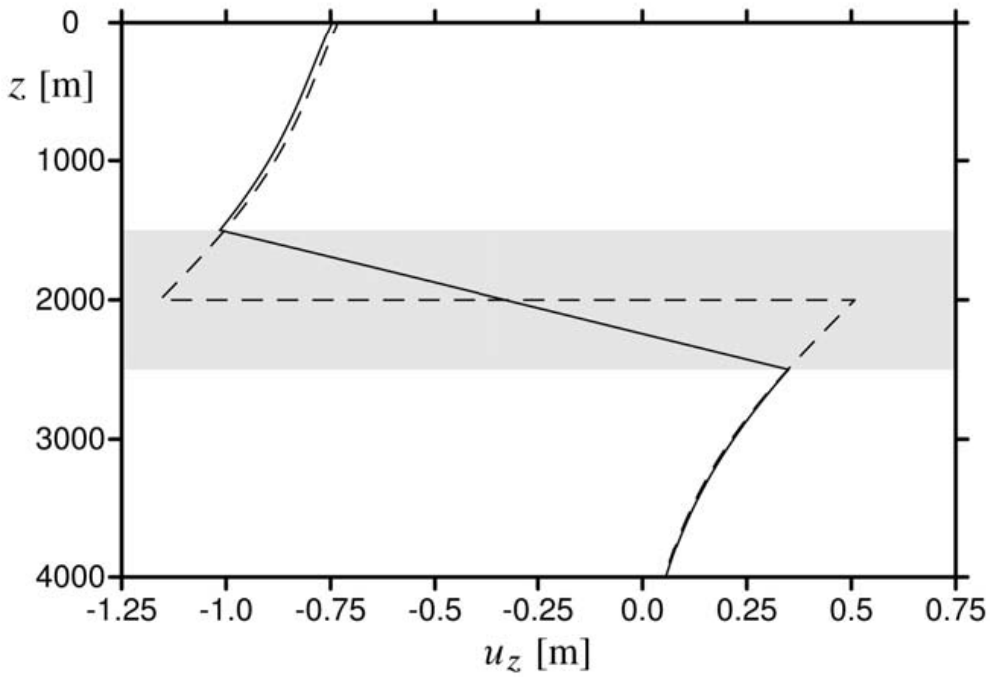

Figure 2.1: Comparison of the vertical displacement at the centre of a disk-shaped reservoir. The Geertsma solution is shown as the dashed line, and the exact solution is the solid line.

Source: (Fjaer, 2008)

As shown in Figure 2.1, the vertical displacement of the center of the disk-shaped reservoir is compared. The Geertsma solution is a dotted line, while the exact solution is a solid line. The gray area represents the reservoir. The difference between the exact solution and the Geertsma solution is small, and most of the difference is concentrated in the reservoir, while outside the reservoir, the difference between the two solutions is very small. This study studies the surface uplift in the CCS project. Using the Geertsma model, a relatively accurate surface displacement can be obtained without elaborate reservoir modeling. It is worth noting that the figure shows the subsidence caused by extraction projects under normal circumstances. To obtain the displacement solution for gas injection projects, that is, CCS projects, it is only necessary to change the sign of the pressure change. The other geomechanical parameters are fixed, as shown in Figure 2.2. The results of the gas injection and extraction projects are symmetrical. Table 6 shows the parameters used in this case.

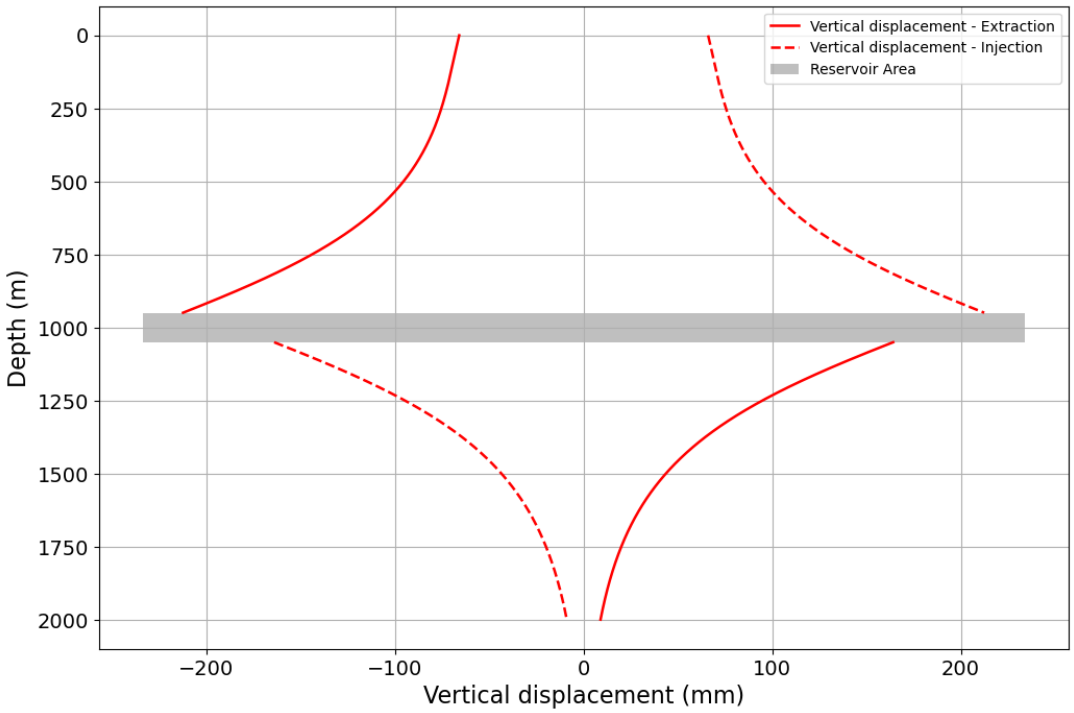

Figure 2.2: Vertical Displacement due to Fluid Extraction and Injection

Parameter	**Value**
Depth to the center of the reservoir [m]	1000
Radius of the reservoir [m]	500
Thickness of the reservoir [m]	100
Poisson's ratio	0.25
Young's Modulus [GPa]	2
Pressure Change [MPa]	±10

Table 2.1: Reservoir properties shown in Figure 2.2.

Table 6 shows the parameters used in this case. These parameters are crucial in the Geertsma model. In addition to explaining how pressure affects surface displacement, they also help us understand the impact of reservoir geometry on surface displacement. Figure 2.3 shows that the larger the ratio of reservoir to burial depth, the greater the ratio of surface subsidence to reservoir compaction, and in CCS projects, the greater the ratio of surface uplift to reservoir expansion.

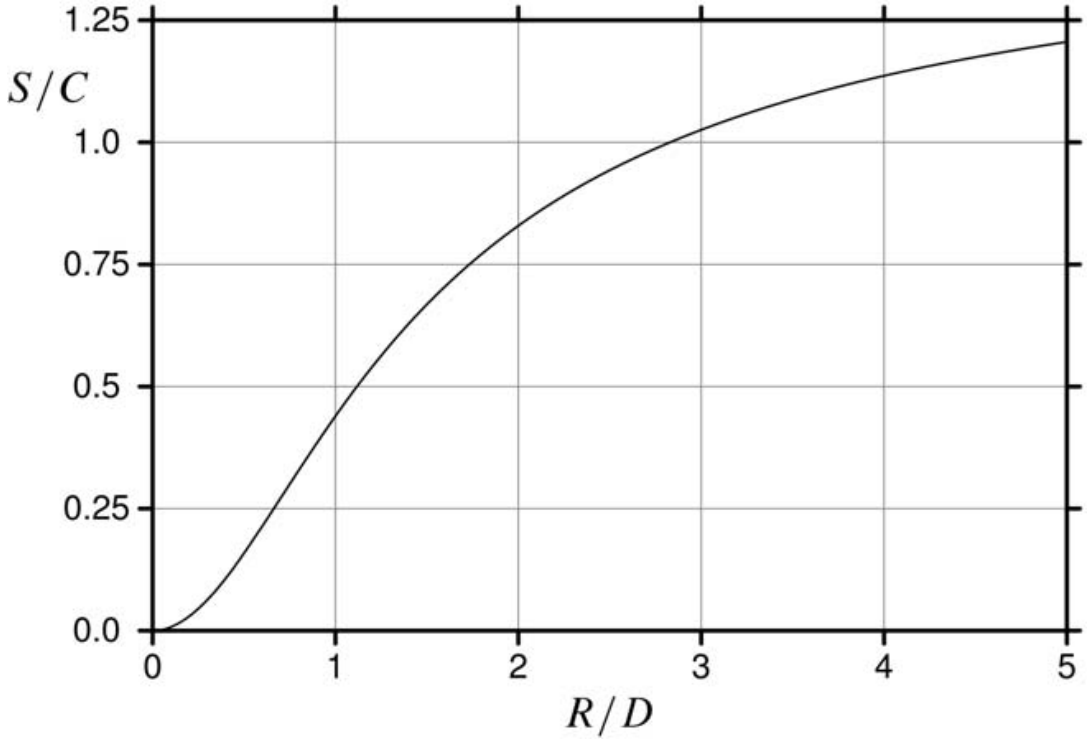

Figure 2.3: Ratio of subsidence S to compaction C as a function of R/D according to the Geertsma model.

Source: (Fjaer, 2008)

2.2 Analytical Formulation and Compaction Coefficient

Stress and strain are two fundamental ideas that are essentially involved in geomechanics concerns. If the cross-sectional area at point (a) is represented as A, and the force acting through this cross-section is denoted as F, then the stress σ at the cross-section is defined as:

$$\sigma = \frac{F}{A} \tag{1}$$

where:

- σ is the stress at the cross-section (Pa),
- F is the applied force (N),
- A is the cross-sectional area (m^2).

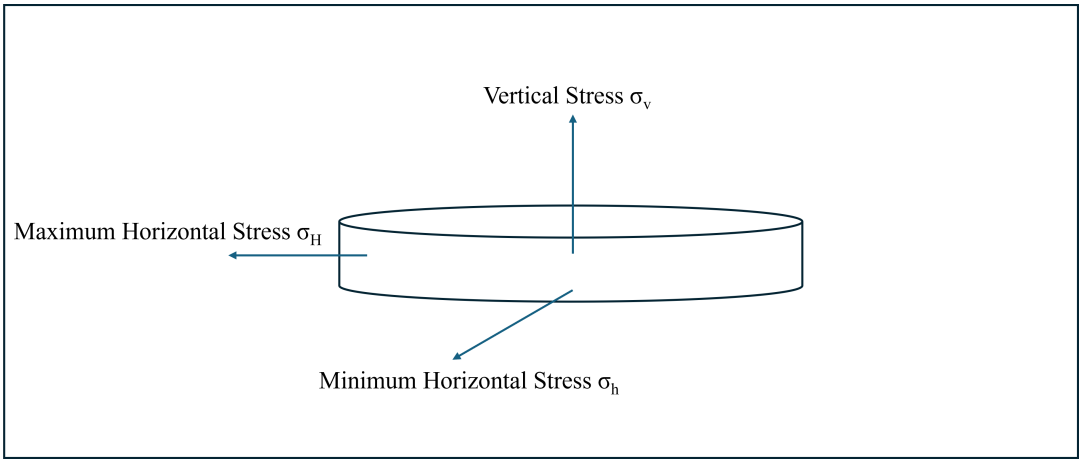

Figure 2.4: Stress Distribution in a Disk-Shaped CCS Reservoir

The stress distribution in the CCS reservoir is shown in Figure 2.4 (modified according to (Fjaer, 2008)). There are three principal stresses, and these stresses correspond to three strains: ε_v, ε_h, and ε_H. The concept of strain originates from Hooke's law, which states that the deformation of an elastic body is proportional to the applied force. This relationship can be expressed as (Rychlewski, 1984):

$$\sigma = E\varepsilon \tag{2}$$

where:

- σ is the applied stress (Pa),
- E is Young's modulus (Pa),
- ε is the strain (dimensionless).

Strain is defined as the relative deformation of a material and is given by:

$$\varepsilon = \frac{\Delta L}{L} \tag{3}$$

where:

- ε is the strain (dimensionless),
- ΔL is the change in length (m),
- L is the original length (m).

The strain formula can be rewritten as:

$$\Delta h = \varepsilon_v h \tag{4}$$

where:

- h is the reservoir thickness (m),
- Δh is the change in reservoir thickness (m),
- ε_v is the vertical strain (dimensionless).

In CCS engineering, reservoir expansion leads to a positive thickness change. To calculate the reservoir expansion, two necessary assumptions must be introduced:

1. The lateral extent of most reservoirs is significantly larger than their thickness. Therefore, we assume that lateral strain is 0, meaning that the reservoir deforms only in the vertical direction. This is referred to as uniaxial compression (expansion).
2. During gas injection, the total vertical stress remains constant.

Terzaghi's effective stress concept provides the relationship between effective stress and total stress, given by (Morita, 2022):

$$\sigma' = \sigma - \alpha P_f \tag{5}$$

where:

- σ' is the effective stress (Pa),
- σ is the total stress (Pa),
- α is the Biot's coefficient (dimensionless, typically between 0 and 1),
- P_f is the pore fluid pressure (Pa).

Combining the above formulas, an equation for calculating the compaction coefficient is obtained, where v is Poisson's ratio.

$$C_m = \frac{1}{E}\frac{(1+\nu)(1-2\nu)}{1-\nu} \tag{6}$$

This is an important formula used in the Geertsma model. When using these equations to calculate surface uplift in CCS projects, there are several points to note. The pressure distribution in the reservoir is usually uneven, and the mechanical properties of different regions in the reservoir are also different. Obtaining reasonable formation parameters is an issue that

needs to be carefully considered in modeling. Although the Geertsma model assumes that the reservoir is homogeneous, it does not mean there is only one parameter to choose when modeling. If we are concerned about the deformation in the center of the reservoir, the typical parameter value of this area instead of the average value of the entire reservoir can be used.

In addition, Young's modulus, mentioned in the formula, refers to the framework modulus, which describes the deformation characteristics of the rock framework itself without including the influence of pore fluid. When modeling, rock parameters measured under dry conditions (in the laboratory) should be used instead of the modulus estimated directly from sonic logging data (Fjaer, 2008; Li, 2016; Morita, 2022).

2.3 DOE and Its Application in Parameter Sensitivity Analysis for CCS Models

Many geological and mechanical input parameters need to be specified when modeling surface uplift in CCS projects. Among these are caprock integrity, reservoir geometry, injection pressure, and formation stiffness. Accurate forecasting and uncertainty quantification depend on an understanding of how these parameters both separately and in combination impact model outputs.

Such multi-parameter studies are made easier by a statistical framework called the Design of Experiments (DOE). DOE investigates combinations of variables to determine their relative influence on responses rather than examining each one separately. Selecting essential variables and their levels, creating a design matrix (such as a full factorial or fractional factorial), running the model, and utilizing methods like ANOVA and regression to analyze output variation are all part of the standard workflow.

DOE is still underutilized in geotechnical and CCS-specific modeling, despite being widely used in engineering fields like aerospace and automotive (Russell, 2018). Its use in this situation provides a methodical way to pinpoint the most important parameters, lower computational expenses, and improve model resilience(Kolivand & Rahmannejad, 2018).

The DOE method includes experimental design methods such as full factorial experimental design, partial factorial experimental design, and orthogonal experimental design but also includes the scientific and effective processing of experimental data using methods such as range analysis and variance analysis after the experiment is completed. The DOE method can study multiple input variables simultaneously and determine the significance of their respective effects on the output variables. Important interactions between input variables can also be evaluated, which are often easily overlooked in experiments using only one factor at a time (Islam & Pramanik, 2016).

Sensitivity analysis refers to determining the degree of influence of each factor on a specified indicator among the many influencing factors of the research object to intuitively observe which factors have an important impact on the indicator and then judge the ability of the research object to resist changes in factors. The DOE method is widely utilized in model sensitivity analysis due to its ability to systematically evaluate the impact of multiple input variables on model performance. The key advantages of DOE in sensitivity analysis are as follows:

1. **Identification of Key Factors:** DOE provides a structured approach to determining which input variables have the most significant influence on model output. This allows researchers to prioritize critical parameters while minimizing unnecessary computational efforts.
2. **Accounting for Interactions:** Unlike traditional methods, DOE captures the interactions between multiple factors.
3. **Enhancing Model Reliability:** By systematically exploring parameter variations, DOE helps identify conditions that may lead to abnormal or unexpected model behavior.

The following section introduces the basic terminology used in the DOE method:

Factor: Represents the input variable of the experiment and the independent variable of the experiment. Factors are divided into digital and textual types. Digital factors are quantified factors, such as the thickness of the reservoir, which can be expressed by specific values; textual factors are qualitative factors that cannot be expressed by specific numbers.

Level: To study the impact of factors on the output results, it is necessary to take two or more values of the factor. These values are called the "level" of the factor, also known as "setting." Variables with only two set values are called two-level variables, which are divided into high level and low level, and the factor center point is located between the high and low levels. The experimental error can be estimated more accurately by setting the center point. Variables with multiple values are called multi-level variables.

Response: Represents the output result of the experiment, that is, the experimental dependent variable. The response can be continuous or discrete. Discrete responses are mostly categories, such as uplift degree (low, medium, high). However, continuous responses are generally more suitable for model sensitivity analysis. The response is expressed by specific numerical

values, which is convenient for range and variance analysis.

2.3.1 Factorial Design

Factorial design is the most commonly used experimental plan to study two or more factors and interaction effects. Factorial design can be divided into full factorial design (FFD) and partial factorial design. Full factorial design means that in this type of experiment, all possible combinations of factor levels are studied, while partial factorial design achieves the purpose of simplifying the experiment by ignoring some unnecessary combinations.

2.3.2 Data Analysis

According to factor design, after the test is completed through model calculation, the results need to be processed through data analysis to obtain the significance of the effect of the desired factor. Data analysis commonly includes range analysis and variance analysis (Verseput, 2000).

The range analysis method is also known as the intuitive or R method. Its calculation method involves determining the factor's influence on the index by calculating the difference between the maximum and minimum values in the average effect. The comparison is made after calculating the range value corresponding to each factor. The larger the value, the greater the factor's influence on the test index. Its advantages are that it is simple, easy to understand, intuitive, and easy to operate. However, when the experimental conditions change and cause data fluctuations, the range analysis cannot determine whether such fluctuations are solely caused by changes in the factor level, and it is easily affected by extreme values and cannot quantitatively estimate the significance of the factor.

The variance analysis method makes up for the shortcomings of the range analysis method. Analysis of variance (ANOVA) is a standard statistical method widely used to evaluate the significance of the influence of one or more factors. It observes the variance of the variables, decomposes the differences and errors caused by the factors on the test indicators, and compares the sum of squares of the between-group and within-group variances. If the difference between the two is large, it indicates that the change in the factor level significantly impacts the indicator (Varanda, Portugal, Ribeiro, Silva, & Silva, 2017). Therefore, to avoid the research results being affected by extreme values and causing large errors.

Factor	Degrees of Freedom (DF)	Sum of Squares (SS)	Mean Square (MS)	F-value	P-value
A	$K_A - 1$	SS_A	MS_A	F_A	P_A
B	$K_A - 1$	SS_B	MS_B	F_B	P_B
C	$K_A - 1$	SS_C	MS_C	F_C	P_C
A*B	$K_A - 1$	SS_{AB}	MS_{AB}	F_{AB}	P_{AB}
A*C	$K_A - 1$	SS_{AC}	MS_{AC}	F_{AC}	P_{AC}
B*C	$K_A - 1$	SS_{BC}	MS_{BC}	F_{BC}	P_{BC}
A*B*C	$K_A - 1$	SS_{ABC}	MS_{ABC}	F_{ABC}	P_{ABC}
Error	$N - K_A$	SS_E	MS_E	-	-
Total	$N - 1$	SS_T	-	-	-

Table 2.2: Standard Analysis of Variance Table

Taking three factors as an example, the standard variance analysis table is shown in Table 2.2. The table involves the following key indicators: **Sum of Squares (SS)**, **Degrees of Freedom (DOF)**, **Mean Square (MS)**, and the related **F-test**. Suppose factor A represents an experimental input variable, such as reservoir thickness. To evaluate the effect of this factor, the sum of squares associated with factor A (SSA) is calculated using the following equation:

$$SS_A = \left(\sum_{i=1}^{K_A} \frac{A_i^2}{n_{Ai}} \right) - \frac{T^2}{N} \tag{7}$$

where:

- SS_A is the sum of squares due to factor A,
- K_A is the number of levels for factor A,

- n_{Ai} is the number of repetitions (trials) at level i of factor A,
- A_i is the sum of response values (e.g., predicted uplift) at level i of factor A,
- T is the total sum of all response values across all experiments.
- N is the total number of experiments

The error sum of squares is calculated as:

$$SS_E = SS_T - (SS_A + SS_B + \cdots) \tag{8}$$

where SS_E represents the error sum of squares. The total sum of squares for all observed values is given by:

$$SS_T = \sum_{i=1}^{N} y_i^2 - \frac{T^2}{N} \tag{9}$$

The DOF and the F-test calculation formulas are as follows:

$$DOF_A = K_A - 1 \tag{10}$$

$$F_A = \frac{MS_A}{MS_E} \tag{11}$$

where:

$$MS_A = \frac{SS_A}{DOF_A} = \frac{SS_A}{K_A - 1} \tag{12}$$

The probability density distribution of F_A can be determined through the model and DOF of error. This is used to further derive the **P-value**. When the **P-value** < 0.05, it indicates that the factor has a significant impact. A smaller **P-value** suggests greater significance, and vice versa.

2.4 Surface Uplift induced by CCS

CO_2 injected into the reservoir will cause the reservoir's deformation, which will be transmitted to the surface layer by layer. If surface uplift is observed, it can indicate that the caprock has been somewhat damaged. Whether the damage is severe depends on the geomechanical parameters of the cap layer. Fractures in the Caprock may cause CO_2 leakage (Zhang et al., 2018). Therefore, monitoring and modeling surface deformation can avoid direct harm caused by surface deformation (damage to buildings, residents, etc.) and warn of other potential risks.

2.5 Innovations and Contributions of This Study

Although many complex numerical simulation software have been used for the geomechanical analysis of CCS projects in recent years, this software usually requires a lot of data and computing resources. This study returns to the classic basic model of Geertsma to evaluate its applicability in multiple actual CCS sites. By comparing the results of the Geertsma model with those of the numerical simulation software (CMG), the feasibility of the Geertsma model in preliminary evaluation is verified, providing an efficient and economical tool for the early design of CCS projects. This study was not limited to a single site, but five different CCS sites were selected for calculation and verification. Through data verification at multiple sites, the performance of the Geertsma model under various geological conditions was comprehensively evaluated. In addition, a sensitivity analysis was performed through a full factorial experimental design to clarify the contribution of each parameter to surface uplift.

3 Methodology

The fundamental mathematical foundations for using the Geertsma model to predict surface displacement brought on by modifications in subsurface conditions are provided by the method covered in this chapter. The displacement equations across a disc-shaped reservoir are derived and integrated to provide a semi-analytical solution to CCS-induced surface uplift. The homogeneity and isotropy assumptions of the model offer a simple yet effective means of assessing displacement patterns. However, because real-world geological formations are so complicated, further confirmation through numerical simulations is necessary.

Furthermore, a full factorial experimental design is used to assess the impact of important geological and operational factors methodically. Finally, data from five representative CCS sites are applied to ensure the model's applicability to varied geological settings.

3.1 Mathematical Derivation and Assumptions of the Geertsma Model

The local variations in strain and stress caused by reservoir compaction do not affect the gravitational stress field. Therefore, in the derivation presented in this report, the influence of gravitational loading is neglected in the calculation and solution process based on Geertsma's strain nucleus theory. For the assumption of a semi-infinite elastic body, the vertical stress on the free surface must be zero. In 1973, Geertsma, utilizing the strain nucleus concept introduced by Mindlin and Cheng, as well as Sen in the theory of thermoelasticity, provided the displacement field expression for the strain nucleus due to compression (Geertsma, 1973) (Mindlin & Cheng, 1950a) (Mindlin & Cheng, 1950b) (Sen, 1951). As shown in Figure 3.1, for a body with volume V, a burial depth D, and pressure drop Δp_f, the elastic displacement in the infinite half-space due to the pressure drop is expressed as:

$$\vec{u} = \frac{C_m}{4\pi}\left\{\frac{\vec{R_1}}{R_1^3} + (3-4\nu)\frac{\vec{R_2}}{R_2^3} - \frac{6z(z+D)\vec{R_2}}{R_2^5} + \frac{2\hat{z}}{R_2^3}\left[(3-4\nu)(z+D)-z\right]\right\} V\alpha\Delta p_f \tag{13}$$

Where:
$\vec{z}$ is the displacement in the z-direction;

z represents the position coordinates in the infinite space where the displacement is calculated;

α is the Biot coefficient, and for weakly consolidated rocks, the typical value is approximately 1, and this paper adopts a value of 1;

C_m is the uniaxial compaction coefficient, defined as:

$$C_m = \frac{1}{E}\frac{(1+\nu)(1-2\nu)}{1-\nu} \tag{14}$$

Here, E and ν are Young's modulus and Poisson's ratio of the reservoir, respectively.

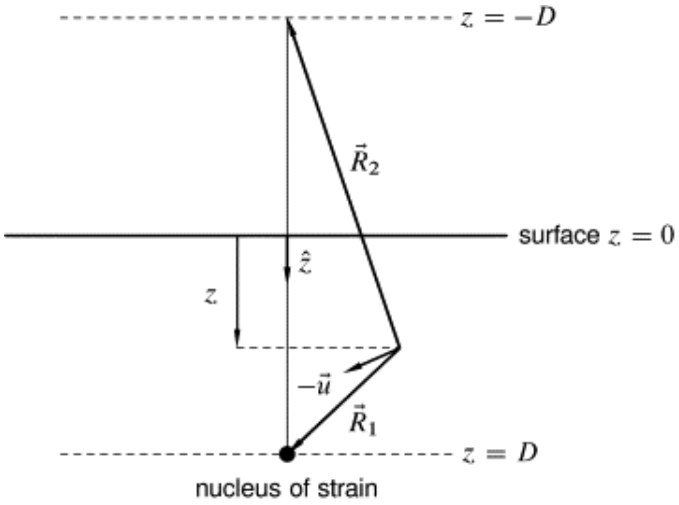

Figure 3.1: Geometry for the Geertsma solution
(Fjaer, 2008)

As shown in Figure 3.1, at any point on the surface of a semi-infinite elastic body ($z = 0$), the following condition is satisfied:

$$\vec{R_1} = \vec{R_2} + 2D\hat{z} \tag{15}$$

By combining Equations 13 and 15, it can be concluded that the displacement vector caused by the nucleus of strain in a semi-infinite elastic body is given by:

$$\vec{u} = \frac{(1-\nu)C_m}{\pi} V \Delta p_f \frac{\vec{R}_1}{R_1^3} \tag{16}$$

It is easy to see from this that the direction of displacement at each point on the surface of the semi-infinite elastic body, caused by the pressure drop Δp_f due to the nucleus of strain, is the same as the direction of vector $\vec{R}_1$.

By decomposing the vector in Equation 13, the displacement at any point within the semi-infinite elastic body induced by the contraction of the nucleus is expressed as:

$$u_z = \frac{C_m}{4\pi}\left[\frac{D-z}{(r^2+(D-z)^2)^{\frac{3}{2}}} - \frac{(3-4\nu)(D+z)}{(r^2+(D+z)^2)^{\frac{3}{2}}} + \frac{6z(D+z)^2}{(r^2+(D+z)^2)^{\frac{5}{2}}} + \frac{2\left[(3-4\nu)(D+z)-z\right]}{\left[r^2+(D+z)^2\right]^{\frac{3}{2}}}\right]\Delta p_f V \tag{17}$$

When $z = 0$, i.e., on the free surface of the semi-infinite elastic body, Equation 17 simplifies to:

$$u_z = \frac{C_m(1-\nu)}{\pi}\frac{D}{(r^2+D^2)^{\frac{3}{2}}}\Delta p_f V \tag{18}$$

Equation 18 is the expression for the displacement at any point on the free surface of the semi-infinite elastic body induced by the pressure drop Δp_f due to the nucleus of strain. This expression can also be obtained by decomposing the vector in Equation 16.

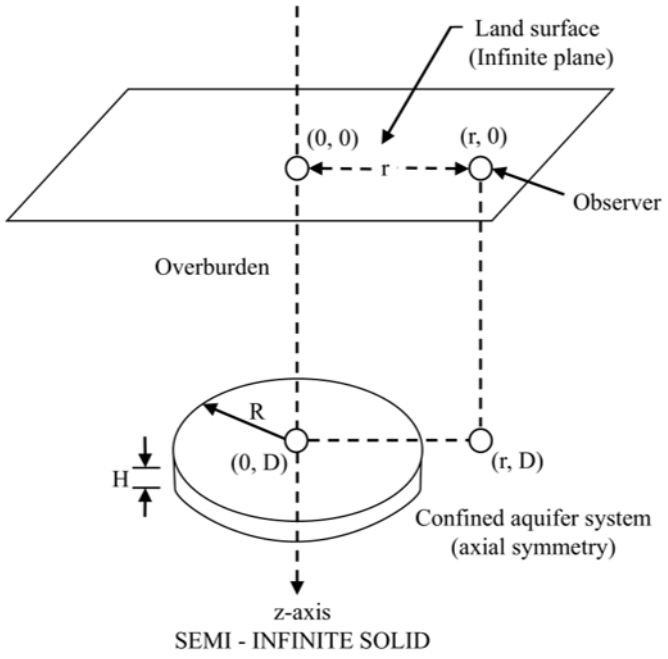

Figure 3.2: Half-space model with a disc-shaped reservoir
(Helm, 1978)

Figure 3.2 shows a half-space model with a disc-shaped reservoir below the surface. After obtaining an equation for the surface displacement due to a nucleus of strain, the surface displacement due to pressure changes within the reservoir can be obtained by integrating the nucleus solution over the entire reservoir volume. Before proceeding with this step, the reservoir and its surroundings must be assumed to be homogeneous, i.e., the uniaxial compaction coefficients and the Poisson's ratios are constant over the entire half-space.After some mathematical variations, an equation for the surface displacement at the surface of a disc-shaped reservoir is finally obtained:

$$u_z(r,0) = -2c_m(1-\nu)\Delta pHR\int_0^\infty e^{-Da}J_1(\alpha R)J_0(\alpha r)\,d\alpha \tag{19}$$

Where:

- $u_z(r,0)$ denotes the vertical displacement at a distance r from the origin on the surface.
- D is the burial depth.
- Δp represents a uniform reservoir pressure reduction/increase.
- H is the thickness of the reservoir.
- R is the radius of the reservoir.
- α is an integration variable that appears in the expression involving Bessel functions.
- J_0 and J_1 are Bessel functions of the first kind of orders zero and one, respectively.

It is important to note that Geertsma gives formulas with a negative sign because Geertsma studies surface subsidence in reservoir engineering. In CCS applications, the final displacement result is positive. It represents surface uplift due to the increased pressure in the reservoir and the positive pressure change. So, the final formula used to calculate surface uplift in CCS only needs to remove the negative sign.

3.2 Introduction to CMG Software and Its Role in Model Validation

CMG is a numerical simulation software widely used in the oil and gas field, CCS, and geothermal energy development. It uses a grid numerical solution to couple the fluid flow simulator GEM with the geomechanical model to obtain the surface displacement (Jun et al., 2023). This study uses CMG-GEM software to verify the Geertsma model. To ensure the reliability of the simulation, this study constructed the Geertsma half-space elastic model and the four-layer geological model based on the actual geological parameters of the In Salah site and compared and analyzed the surface uplift results obtained by the two.

CMG-GEM uses the coupling method to solve CO_2 flow and reservoir deformation. The calculation process is as follows (Khan, Khulief, Al-Shuhail, Bashmal, & Iqbal, 2020):

(1) CO_2 Flow Equations The mass conservation equation for CO_2 transport in porous media is:

$$\frac{\partial}{\partial t}(\rho_f\phi) + \nabla\cdot(\rho_f q) = Q_m \tag{20}$$

where ρ_f is the CO_2 density, ϕ is porosity, q is Darcy's velocity, and Q_m is the mass source term.
CO_2 flow follows Darcy's law:

$$q = -\frac{k}{\mu}(\nabla p_f + \rho_f g\nabla D) \tag{21}$$

where k is permeability, μ is viscosity, and p_f is pore pressure. The pore pressure distribution obtained from these equations influences the geomechanical response.

(2) Deformation Equations Reservoir deformation is governed by the stress equilibrium equation:

$$-\nabla\cdot\sigma = F_v = \rho_{\text{avg}}g \tag{22}$$

where σ is the stress tensor and ρ_{avg} is the average rock density.
The stress-strain relationship follows:

$$\sigma - \sigma_0 = C:(\varepsilon - \varepsilon_0 - \varepsilon_{\text{inel}}) - \alpha p_f I \tag{23}$$

where C is the elastic coefficient matrix, α is the Biot coefficient, and ε is the strain tensor. The strain tensor is defined as:

$$\varepsilon = \frac{1}{2}((\nabla u)^T + \nabla u) \tag{24}$$

where u represents the displacement field. The vertical displacement component u_z obtained from solving these equations corresponds to the predicted surface uplift.
CMG provides a variety of coupling methods to couple the fluid module and the geomechanics module. This study chooses to use one-way coupling. The schematic diagram of one-way coupling is shown in Figure 3.3. One-way coupling does not

consider the impact of the geomechanics module on the fluid module, and is more effective when only focusing on geomechanics problems.

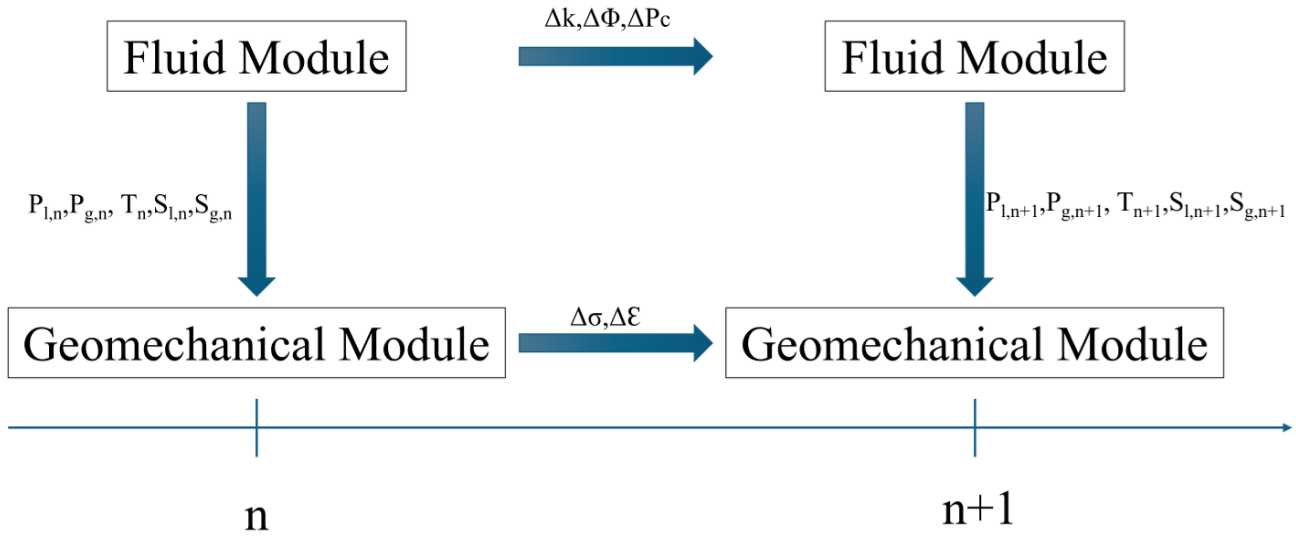

Figure 3.3: Principle diagram of one-way coupling

3.3 Full Factorial Experimental Design

A full factorial experimental design is a statistical method used to study the effects of multiple factors on an outcome variable. In a full factorial design, each factor is tested at two or more levels, and all possible combinations of factor levels are considered. This comprehensive approach enables researchers to evaluate not only the individual (main) effects of each factor but also their interaction effects (Wikipedia, 2025).

For this study, a full factorial design is employed to assess the sensitivity of the Geertsma model to its six key parameters. Given that the Geertsma model includes six factors, each with two levels, a $2^6 = 64$ combination experimental setup is required. These factors include:

- Pressure change (ΔP)
- Young's modulus (E)
- Poisson's ratio (ν)
- Depth (D)
- Reservoir radius (R)
- Layer thickness (H)

The selection of parameter levels is based on actual field data from CCS sites, ensuring practical relevance in the sensitivity analysis.

3.3.1 Experimental Factor Levels

Table 3.1 presents the high and low levels assigned to each parameter in the Geertsma model. These levels represent the values observed in actual CCS sites.

Factors / Level	Low	High
Pressure Change (ΔP) [MPa]	0.02	**7**
Young's Modulus (E) [GPa]	2.1	**25**
Poisson's Ratio (ν)	0.2	**0.31**
Depth (D) [m]	800	**3250**
Reservoir Radius (R) [m]	400	**5000**
Layer Thickness (H) [m]	20	**676**

Table 3.1: Full factorial experiment design setup

Each of these factors influences the predicted surface uplift, making it crucial to analyze their individual and interactive effects.

3.3.2 Data Collection and Analysis

For each experimental combination, the surface uplift curve is recorded. The response variables used for analyzing the model sensitivity are:

- **Maximum uplift** ($u_{\max}$): The displacement at the center of the surface ($r = 0$). This measures the extreme effect of the parameters.
- **Area Under the Curve (AUC)**: The integral of the uplift profile, which quantifies the overall surface deformation.

These response variables help assess the relative influence of each parameter on surface uplift, providing a quantitative basis for identifying key sensitivity factors.

3.3.3 Sensitivity Analysis Methods

To evaluate the effect of each parameter on surface uplift, sensitivity analysis is performed using the **effect estimate method**. The influence of each factor is computed as:

$$\text{Effect of Factor A} = \frac{1}{N}\left(\sum \text{Response at High Level} - \sum \text{Response at Low Level}\right) \tag{25}$$

where N is the total number of experiments.
The significance of each effect is assessed using the standardized effect formula:

$$SE_{\text{Effect}} = \frac{\text{Standard Deviation of Residuals}}{\sqrt{N}} \tag{26}$$

$$\text{Standardized Effect} = \frac{\text{Effect Estimate}}{SE_{\text{Effect}}} \tag{27}$$

Higher standardized effects indicate that the corresponding parameter has a significant impact on surface uplift.

3.3.4 Implications of Sensitivity Analysis

The results from sensitivity analysis will help identify the most influential factors in the Geertsma model. The key findings include:

- Identifying parameters with the largest contribution to surface uplift variation.
- Understanding the interactions between different parameters.
- Providing insights for optimizing model assumptions and parameter selection for CCS applications.

By employing a full factorial experimental design and sensitivity analysis, this study systematically evaluates the dependence of surface uplift on key geological and mechanical parameters, leading to improved predictions in CCS site modeling.

3.4 Geological and Geomechanical Parameter Sources for Each CCS Site

The Geertsma model has been applied to real-world carbon storage projects using data from five existing carbon storage sites. These locations include Saskatchewan fields, Sleipner, Weyburn, Gundih, and Salah. Publicly available literature provided these locations' geology and injection parameters, and subsurface modeling and analysis were conducted using the documented values. This work ensures that the surface uplift estimates and sensitivity analysis still apply to real-world CCS applications by integrating field data.

Field	Layer thickness (m)	Depth (m)	Reservoir radius (m)	Poisson's ratio	Young's Modulus (GPa)	Pressure Change (MPa)	Max Surface Uplift (mm)
In Salah Field	20	1800	5000	0.2	6	7	25 (J. Rutqvist et al., 2011)
Sleipner Field	250	800	5000	0.24	2.1	0.1	No significant surface deformation (J. P. Verdon et al., 2013)
Weyburn Field	75	1425	2000	0.31	14.5	6.28	No reported uplift
Gundih Field	676	1000	1000	0.25	18.24	0.02	0.2 (Suhendi et al., 2019)
Saskatchewan Field	60	3250	5000	0.27	25	1	16 (Samsonov et al., 2015)

Table 3.2: Geological parameters of the five CCS sites

The values in Table 3.2 were extracted from peer-reviewed studies that have conducted detailed subsurface characterization and geomechanical modeling of these CCS sites. These studies have used the reported parameters for numerical modeling, history matching, and field monitoring(J. Rutqvist et al., 2002; J. P. Verdon et al., 2013; Zweigel et al., 2004; Samsonov et al., 2015; Suhendi et al., 2019; A. R. Asikin et al., 2018). The selection of these specific CCS sites is based on:

- Their well-documented geological properties in published literature.
- The availability of geological and pressure data, allowing for realistic modeling.
- Their relevance to surface uplift studies, as they include varying geological conditions and injection scenarios.

By using these data, the Geertsma model can be applied to real CCS conditions, ensuring that the sensitivity analysis results are both scientifically rigorous. Table 3.2 shows that the parameters of several locations varied significantly from one another. The results might not be comparable if the surface uplift of each site is directly compared. The displacement of several sites can be compared on the same scale without being impacted by the actual scale (such as reservoir thickness, radius, etc.) by normalizing the surface displacement and turning it into a relative number. The following is the normalizing formula:

$$r_{\text{normalized}} = \frac{r}{R} \tag{28}$$

$$uz_{\text{normalized}} = \frac{uz}{C_m \cdot h \cdot \Delta p} \times 100 \tag{29}$$

The Geertsma model used in this study predicts surface uplift, and its accuracy depends mainly on the input geological and geomechanical parameters. Therefore, this section will provide detailed sources and a selection basis for the study's parameters of the five CCS sites. Due to the significant differences between the site's geological and injection conditions, selecting these parameters is directly related to the rationality and comparability of the model prediction results.

The parameters listed in Table3.2 have been strictly selected, and the sources include drilling reports, laboratory core tests, seismic exploration data, and existing numerical simulation studies. To ensure the scientificity and repeatability of the model results, the selected parameters must be consistent with the actual geological scene and represent the typical characteristics of the site. In addition, try to select parameter values that have been repeatedly used in related studies or numerical simulations to ensure the reliability of the parameters.

3.4.1 In Salah Field

The geological and geomechanical parameters of the In Salah site are mainly derived from the reservoir and geomechanical coupling simulation study conducted by Rutqvist et al. (J. Rutqvist et al., 2011)for the area. The study lists the lithology and rock mechanical parameters of each stratum in detail (Table 3.3), and these data are widely used in subsequent numerical simulations and actual field history matching.

Layer	Shallow overburden (0–900 m)	Caprock (900–1800 m)	Injection zone (1800–1820 m)	Base (below 1800 m)
Lithology	Cretaceous sandstones and mudstones	Carboniferous mudstones	Carboniferous sandstone (C10.2)	Mudstone (D70)
Young's modulus, E (GPa)	1.5	20	6	20
Poisson's ratio, ν (–)	0.2	0.15	0.2	0.15
Effective porosity, ϕ (–)	0.1	0.01	0.17	0.01
Permeability, k (m^2)	1×10^{-17}	1×10^{-21}, 1×10^{-19}	1.3×10^{-14}	1×10^{-19}
Residual gas (CO_2) saturation (–)	0.05	0.05	0.05	0.05
Residual liquid saturation (–)	0.3	0.3	0.3	0.3
Van Genuchten (1980), P_0 (kPa)	19.9	621	19.9	621
Van Genuchten (1980), m (–)	0.457	0.457	0.457	0.457

Table 3.3: Material properties used in the modeling CO_2 injection at In Salah.

Source: (Fjaer, 2008)

Specifically, the reservoir Young's modulus used in this study is 6 GPa, which comes from the laboratory rock mechanics test of the C10.2 reservoir core in the In Salah area conducted by Liverpool University and verified by well logging data. The Poisson's ratio is selected as 0.2, which is also determined based on the results of the laboratory core test. The reservoir thickness (20 m) and burial depth (1800 m) are directly determined based on the field drilling data, and the reservoir burial depth range is confirmed to be the Carboniferous sandstone stratigraphic unit of 1800–1820 m. The value of the reservoir radius (5000 m) comes from the numerical simulation of geomechanics of the site by Verdon et al. (J. P. Verdon et al., 2013). After numerical model calibration, it is an empirical setting value that can better reflect the observed surface deformation range and spatial distribution characteristics.

The pressure change value (7 MPa) used in this study comes from the actual field observation data and history matching analysis results, representing the typical pressure change amplitude observed in the reservoir five years after CO_2 injection. Therefore, the above parameters were selected in this study, mainly because these data are derived from field observations and laboratory tests and have been widely verified by previous studies. They have high credibility and representativeness and are suitable for the surface uplift prediction analysis of the Geertsma model.

3.4.2 Sleipner Field

Existing field geological surveys, numerical simulation studies, and laboratory test results were used to determine the geological and geomechanical parameters of the Sleipner site. The numerical simulation studies published by Audigane et al. and Frangeul et al. (Audigane, Gaus, Czernichowski-Lauriol, Pruess, & Xu, 2007; Frangeul, Nghiem, Caroli, & Thibeau, 2004), which carried out stratigraphic definition and stratification based on field drilling and seismic exploration data of the Utsira sandstone aquifer, were specifically used to determine the reservoir thickness (250 m) and depth (800 m). The reservoir radius (5000 m) was set as the theoretical value of the model input to effectively cover the larger geological spatial scale (Guilherme) of the study area (da Fontoura, 2016). The Poisson's ratio (0.24) and Young's modulus (2.1 GPa) were selected based on the core mechanics experiments and logging data analysis results of the Utsira sandstone in the studies of Baklid et al. and Chadwick et al. (Baklid, Korbol, & Owren, 1996), which are widely used in geomechanical simulations of the Utsira reservoir.

The reservoir pressure change (0.1 MPa) is cited from the research results of Chadwick et al. (Chadwick, Williams, Williams, & Noy, 2012). By analyzing time-lapse seismic velocity changes, they calculated that the actual pressure change in the reservoir was less than 0.1 MPa. Considering the conservative low rock velocity sensitivity case, the maximum reservoir pressure change does not exceed 0.17 MPa. Therefore, this study selected 0.1 MPa as the model input value to more accurately reflect the actual pressure change level of the reservoir after injection.

3.4.3 Weyburn Field

The model parameters of the Weyburn site are mainly derived from geological model parameters in other literature. Jafari et al. provided detailed data on the Weyburn reservoir, which provided the core input parameters for the Geertsma model (Jafari, Talman, & Perkins, 2011). The reservoir thickness was set at 75 meters, and the burial depth was 1425 meters. These data were derived from on-site drilling and geological exploration. The Young's modulus and Poisson's ratio of the reservoir (14.5 GPa and 0.31, respectively) were derived from Verdon's research, which specifically conducted rock mechanics experimental analysis in the Weyburn area (J. Verdon, 2011). The reservoir radius was set at 2000 meters. Based on the research of Khazaei et al. (Khazaei & Chalaturnyk, 2017), this paper modeled the reservoir at the Weyburn site and gave accurate reservoir radius data. The catalytic pressure change was 6.28 MPa, derived from Jafari's research and inferred through historical matching (Jafari et al., 2011).

3.4.4 Gundih Field

According to the literature on the Gundih area (Suhendi et al., 2019; A. Asikin, Sule, Priyono, Tsuji, & Raharjo, 2015), the geological parameters of the area were obtained through seismic data and well logs. These data provide the basis for the construction of the model and can accurately reflect the mechanical properties of the formations in the area. In addition, the reservoir radius used in the Geertsma model is a parameter of the Gundih area model in this study. The pressure changes are the results of the numerical simulation of this study.

3.4.5 Saskatchewan Field

The study of the Saskatchewan site directly provided most of the reservoir parameters in the area (Samsonov et al., 2015). The Poisson's ratio and Young's modulus of the reservoir were obtained from well data. This study used the Mogi model to calculate the surface uplift, the burial depth, and the thickness of the reservoir, which are all from the parameters of the Mogi model. This model simplifies the spatial characteristics of the reservoir, and the influence of the reservoir radius is ignored. This paper will use different radii to analyze the results. The pressure changes calculated using the model in the literature are used as parameters of the Geertsma model.

4 Sensitivity Analysis

This chapter aims to explore the impact of different parameter changes in the Geertsma model on the surface uplift prediction results. In order to systematically analyze the role of each major geological and mechanical parameter, this study adopts a full factorial experimental design method, sets two levels for each of the six key parameters, and constructs a total of 64 sets of parameter combinations (Table 3.1).

In the analysis of this chapter, these 64 sets of simulation results will be compared, focusing on the maximum surface uplift value and its spatial distribution. By comparing the simulation results under different combinations, the parameters that have the most significant impact on the model response can be identified. In addition, for some results, simple statistical methods (such as response range comparison and contribution rate estimation) are also combined to further explore parameter sensitivity. The next section will give Figures and summary tables to support subsequent analysis and discussion.

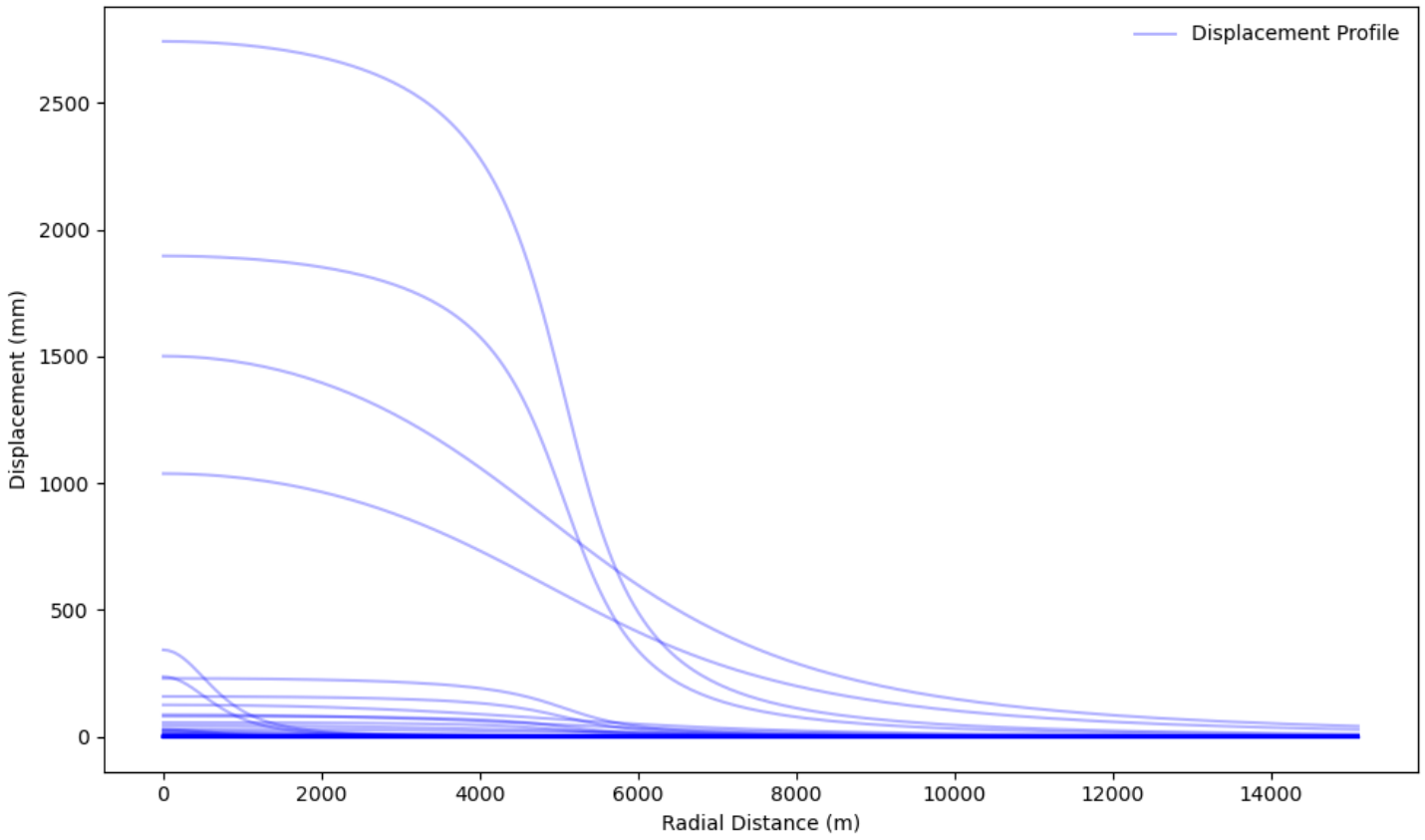

Figure 4.1: Displacement profile for all factorial analysis runs

Figure 4.1 shows the distribution of surface uplift calculated under 64 different parameter combinations. The horizontal axis represents the radial distance, and the vertical axis represents the surface displacement. Different curves represent the distribution of surface displacement under different parameter combinations. The surface displacement reaches the maximum value above the reservoir center, then gradually decreases with the increase of radial distance, and finally tends to zero. This distribution trend is consistent with the geological deformation theory; the influence range of formation deformation is limited, and its influence gradually decreases with the increase of distance from the center.

Under some parameter combinations, the maximum surface uplift can reach 2.5m, which is much higher than the uplift level generally observed in CCS projects. However, under most parameter combinations, the maximum surface displacement is much lower than 2.5m, which indicates that only a few extreme cases will cause such significant surface uplift. Therefore, to conduct sensitivity analysis more effectively, a threshold is set to filter out some extreme cases.

In some cases, the peak of the curve is low, and the change is gentle, while in other cases, the peak of the curve is high and decays rapidly in a short distance. Although some studies have observed meter-scale surface subsidence in some geological engineering projects, there is no literature report on the actual observation of such a considerable surface uplift in the CCS case. This indicates that some extreme parameter combinations may not conform to the actual situation, and it is necessary to screen a reasonable range of geomechanical parameters to ensure the credibility of the simulation results.

In addition, this abnormally large surface uplift may suggest some extreme geological conditions, such as abnormally high elastic response of the reservoir. This study will filter out the combinations that cause a maximum uplift of more than 1m. The four combinations that cause the maximum uplift of more than 1m are shown in Table 4.1.

Factor	Pressure	Young's modulus	Poisson's ratio	Depth	Radius	Thickness	Maximum uplift (mm)
Combination 1	7.0	2.1	0.2	800	5100	676	2741.96
Combination 2	7.0	2.1	0.31	800	5100	676	1895.76
Combination 3	7.0	2.1	0.2	3250	5100	676	1501.01
Combination 4	7.0	2.1	0.31	3250	5100	676	1037.78

Table 4.1: Parameter combinations that result in a maximum uplift of more than 1000 mm

The exact parameters of these combinations are pressure change, Young's modulus, reservoir radius, and reservoir thickness. It can be preliminarily considered that these parameters are important factors leading to large surface uplift. The different variables in the four combinations are Poisson's ratio and reservoir burial depth. The extreme uplift may be mainly caused by high pressure and low reservoir stiffness of 2.1 GPa, while the changes in burial depth and Poisson's ratio may have relatively small effects on surface uplift. It is reasonable to filter these parameter combinations because such large surface uplift is usually not observed in CCS projects. These parameter combinations are too extreme and do not conform to the physical properties of actual CCS reservoirs.

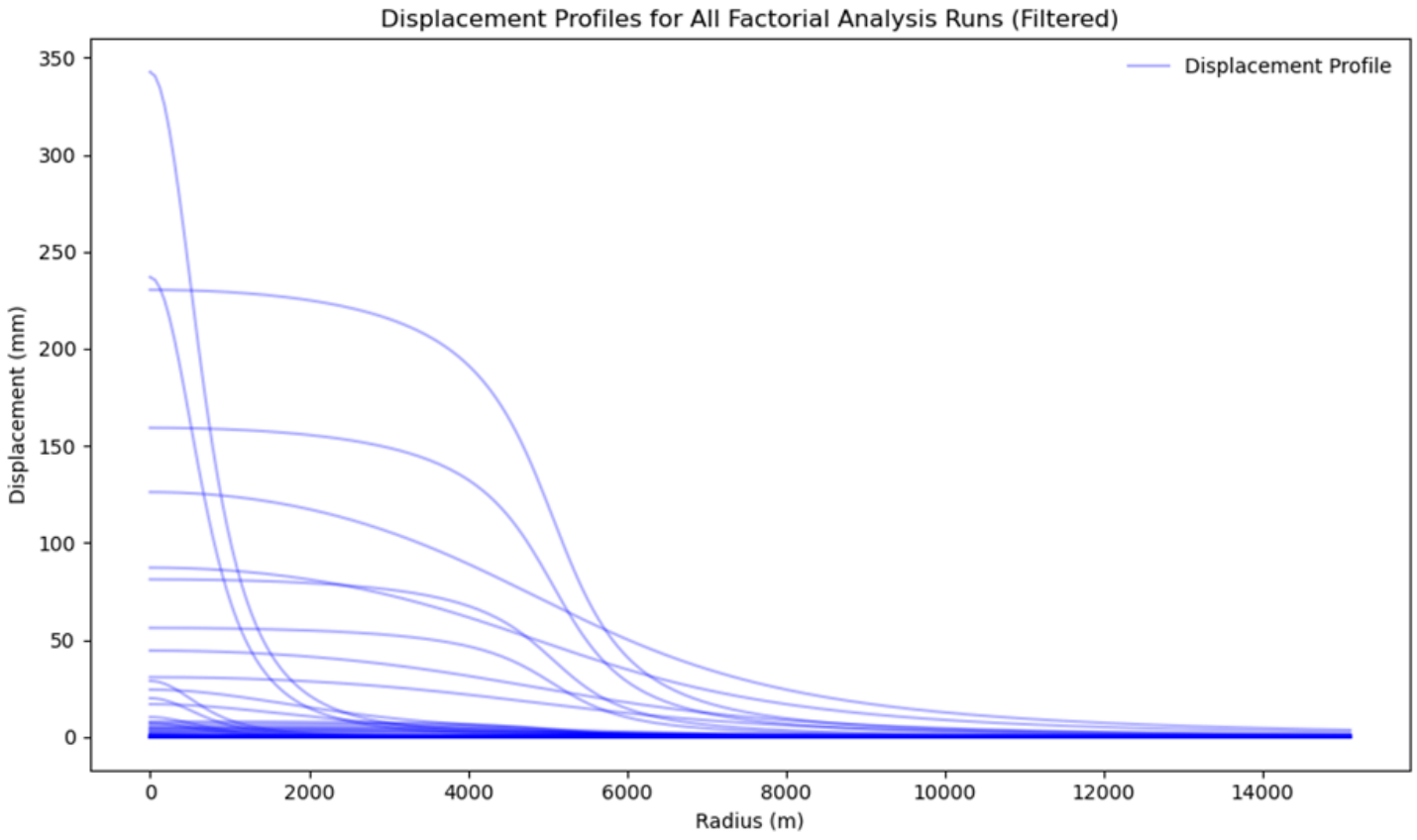

Figure 4.2: Displacement profile with a maximum uplift of less than 1m

Figure 4.2 shows the distribution of surface uplift after screening. Compared with the previous unscreened data (maximum uplift of 2.5m), the uplift results that are too large have been eliminated. After screening, the maximum surface uplift is reduced to 350 mm, an order of magnitude lower than the previous 2.5 m. The surface uplift of most cases is small, most of which are less than 10 mm, and only a few cases exceed 100 mm, which is more in line with the observed CCS-related surface deformation magnitude. Using this simulation result for subsequent analysis will produce more reasonable and realistic results.

Factor	Pressure	Young's modulus	Poisson's ratio	Depth	Radius	Thickness	Maximum uplift (mm)
Combination 1	7.0	2.1	0.2	800	400	676	342.56
Combination 2	7.0	2.1	0.31	800	400	676	236.84
Combination 3	7.0	25.0	0.2	800	5100	676	230.32
Combination 4	7.0	25.0	0.31	800	5100	676	159.24
Combination 5	7.0	25.0	0.2	3250	5100	676	126.08

Table 4.2: Parameter combinations that result in a maximum uplift of more than 100 mm

Table 4.2 shows the parameter combinations that lead to a maximum uplift greater than 100 mm. Combined with Table 4.1, some preliminary conclusions can be drawn. The pressure of all combinations is 7.0 MPa. Pressure may be the dominant factor affecting surface uplift.

4.1 Sensitivity Analysis of Maximum Surface Uplift

The maximum surface uplift reflects the strongest influence of different model parameters on surface deformation. The surface uplift calculated by the Geertsma model is nonlinear, so focusing on one parameter first can make the sensitivity analysis more efficient. The effect of each factor and interaction factor is calculated using the formula mentioned in Chapter 3.3.3, and the results are shown in Figure 4.3.

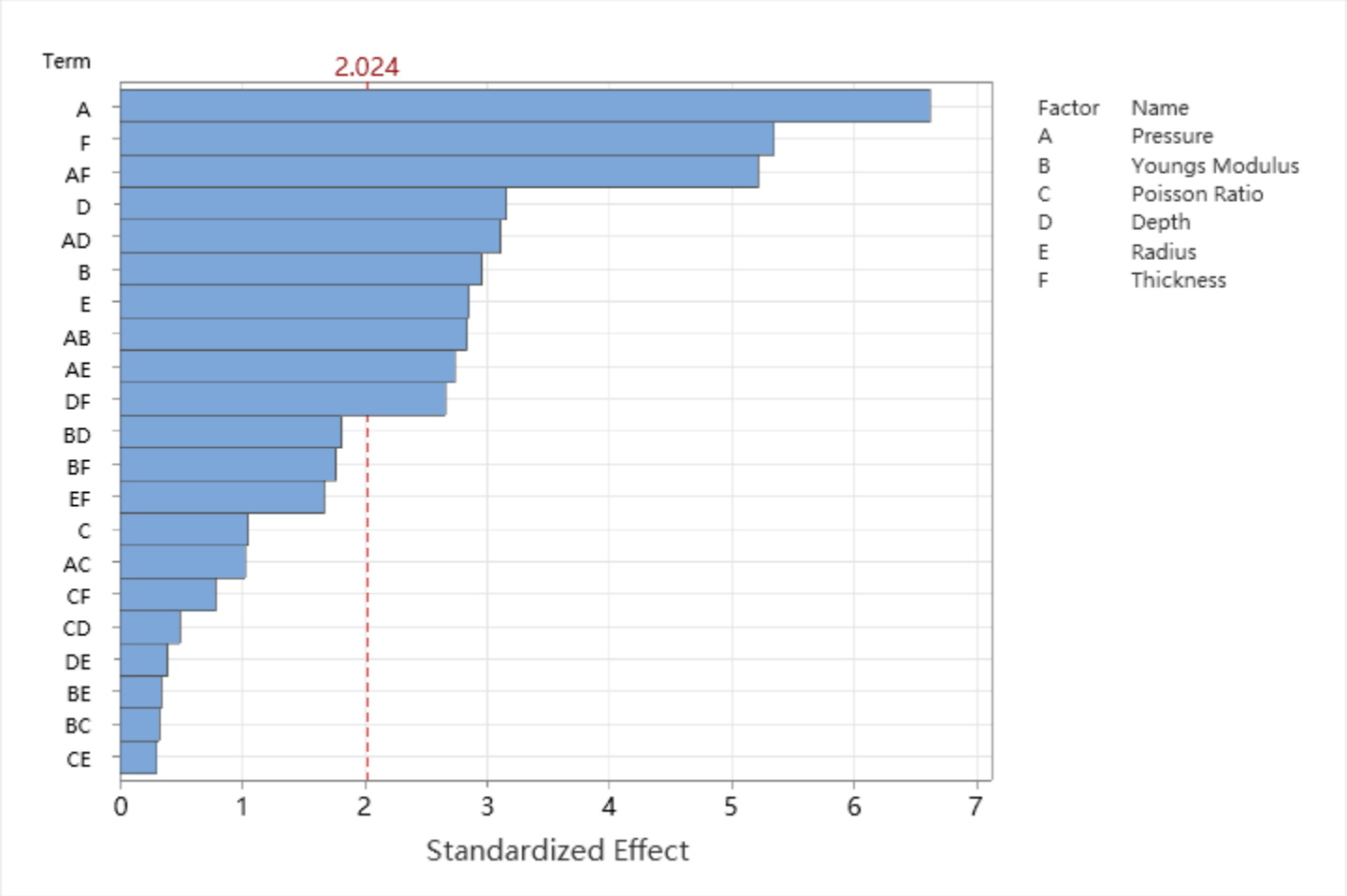

Figure 4.3: Pareto Chart of effects of model parameters on maximum uplift

As shown from the Pareto chart in Figure 4.3, pressure and thickness are the two most important factors affecting the maximum surface uplift. Among them, the standardized effect value of pressure is the highest, indicating that it has the most significant impact on the maximum surface uplift. An increase in reservoir pressure change usually leads to a greater surface uplift. Secondly, thickness is also a key factor. Thicker reservoirs may cause more obvious surface deformation. In addition, the interaction between pressure and thickness (AF) also has a significant effect, indicating a coupling relationship between these two parameters, which may amplify or weaken the impact when they act alone. In contrast, factors such

as depth and Young's modulus have a smaller impact on the maximum surface uplift but still have a specific contribution. The impact of Poisson's ratio and some second-order interaction terms is weaker and is below the significance threshold (red dotted line).

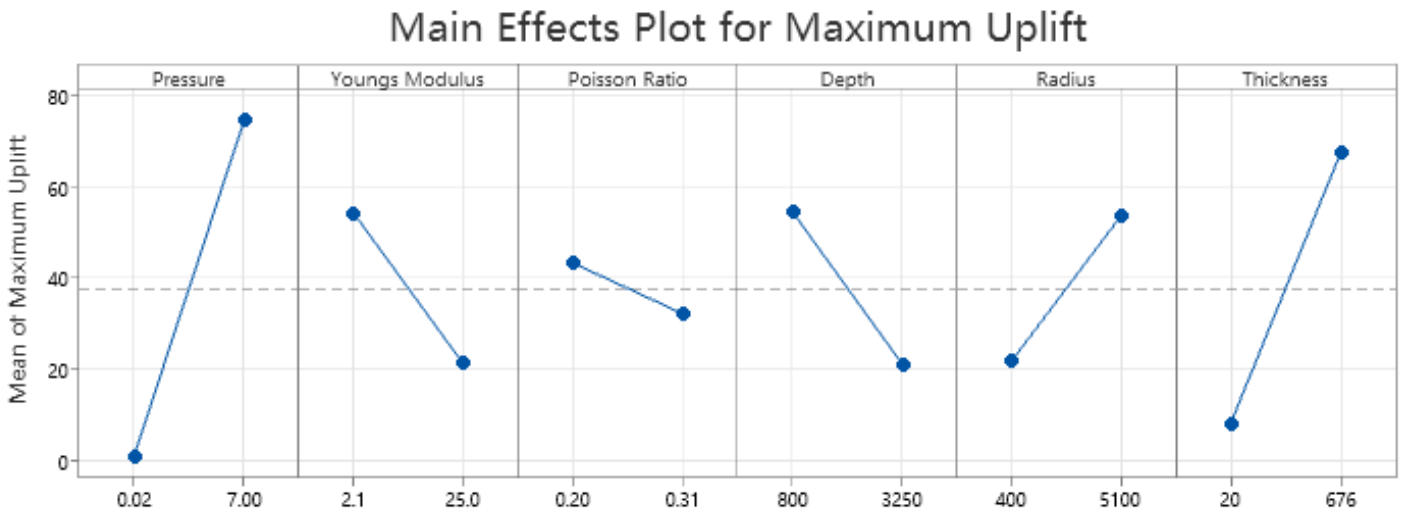

Figure 4.4: Main Effects Plot for Maximum Uplift

Figure 4.4 shows the main effect diagram of the maximum surface uplift, from which we can see the independent effects of different model parameters on the surface uplift. Pressure change and thickness have the most significant effects on the maximum surface uplift, and both show a clear positive correlation; that is, with the increase of pressure change and thickness, the surface uplift increases significantly. In particular, the effect of pressure change is particularly prominent. The maximum surface uplift is almost zero at low pressure, and when the pressure increases to the highest value, the surface uplift reaches the maximum. Young's modulus shows a negative correlation trend. A larger Young's modulus will reduce the surface uplift, consistent with the physical property that increased formation stiffness leads to reduced deformation. The effect of Poisson's ratio is relatively gentle, and the overall change is insignificant, indicating that this parameter has a relatively small effect on the surface uplift. Depth shows a negative correlation. Deeper reservoirs will lead to smaller surface uplift, possibly due to the enhanced constraint effect of deeper formations on deformation. The influence of the radius on surface uplift is more complex. Although it shows an overall upward trend, the change is small. In summary, pressure and thickness are the key factors affecting the maximum surface uplift, while the influence of parameters such as Young's modulus, depth, and radius is relatively small but still cannot be ignored. These results further confirm the conclusion of the Pareto chart analysis in Figure 4.3.

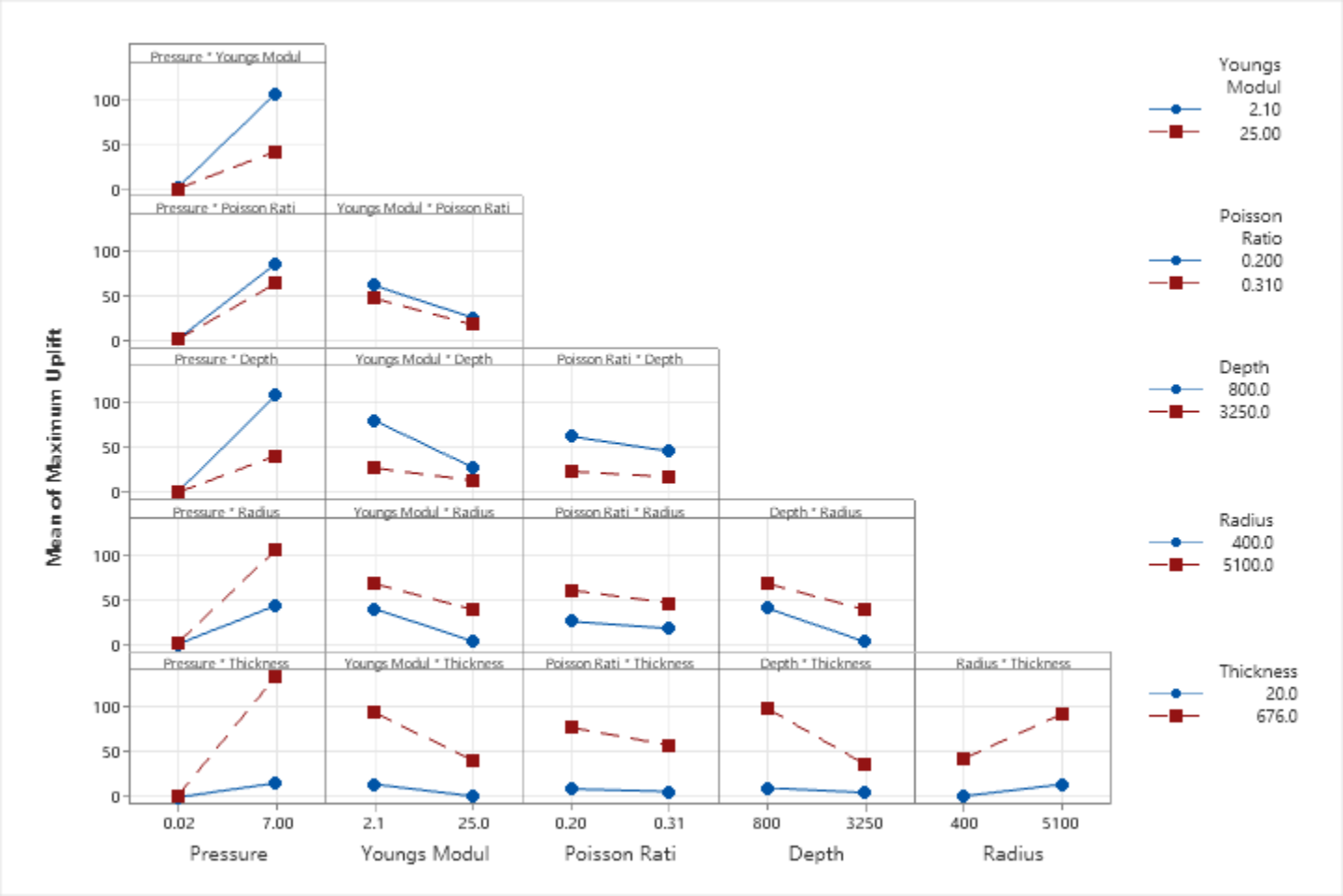

Figure 4.5: Interaction Plot for Maximum Uplift

Figure 4.5 shows the interactive effects of different model parameters on the maximum surface uplift. As can be seen from the figure, the interaction between pressure change and other parameters is the most significant, especially when combined with reservoir thickness and Young's modulus, the change of surface uplift is the most obvious. The interaction between pressure and Young's modulus shows that at higher pressures, a smaller Young's modulus leads to greater surface uplift, which is consistent with the physical property that lower stiffness materials are more easily deformed. Similarly, the interaction between pressure and thickness shows that greater reservoir thickness further enhances surface uplift under high pressure changes.

In addition, the interaction between depth and other parameters is usually negatively correlated, that is, as the reservoir depth increases, the overall trend of surface uplift decreases. For example, in the interaction diagram of depth and thickness, the deeper reservoir has a smaller increase in surface uplift even at a greater thickness, indicating that depth may have a certain constraint on uplift. The interactions of Young's modulus, Poisson's ratio, and radius are relatively weak, but some trends can still be observed, such as a larger Young's modulus generally reduces uplift, while a larger radius may slightly increase uplift, but not as much as pressure and thickness.

These interactions demonstrate that pressure changes and thickness continue to be the main factors influencing the maximum surface uplift, with their trends remaining consistent across various parameter combinations. The interaction of parameters like depth and Young's modulus may further alter the specific magnitude of surface uplift.

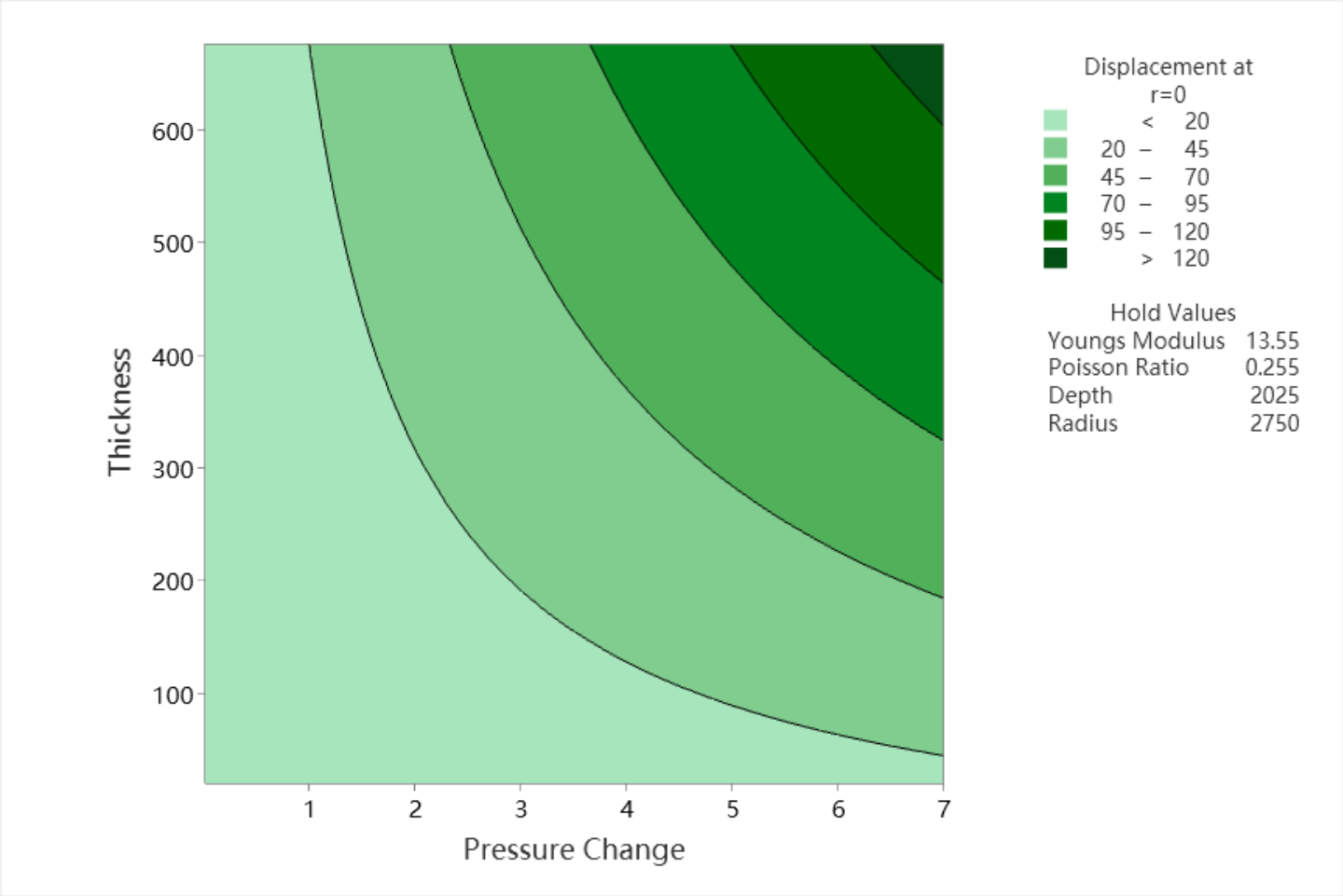

Figure 4.6: Contour Plot of Maximum Uplift vs Thickness, Pressure Change

By fixing the Young's modulus, Poisson's ratio, reservoir depth, and radius at certain values and drawing contour maps of the two main variables, thickness and pressure change, interference from other factors can be avoided. As shown in Figure 4.6, the effect of pressure change on surface uplift is particularly obvious: it can be observed that when the pressure change is small, such as in the range of 1-2 MPa, the increase in reservoir thickness has limited effect on the maximum surface uplift; but as the pressure change increases to higher levels such as 6-7 MPa, the maximum surface uplift increases rapidly even if the reservoir thickness does not change much, indicating that pressure change plays a dominant role in the surface uplift predicted by the model.

Similarly, the contour map illustrating factors with minimal impact on maximum surface uplift, specifically reservoir radius and Poisson's ratio, can be drawn as shown in Figure 4.7. According to the conclusions of the sensitivity analysis, the influence of Poisson's ratio and reservoir radius on the maximum surface uplift is considerably smaller than that of pressure change and reservoir thickness, which is reflected in this figure. The contour line trends show that the maximum surface uplift increases with the reservoir radius. Specifically, as the reservoir radius increases from 1000 meters to 5000 meters, the magnitude of surface uplift rises from less than 30 mm to more than 60 mm. This indicates that increasing the reservoir radius expands the affected region, thereby moderately enhancing the maximum surface uplift at the center.

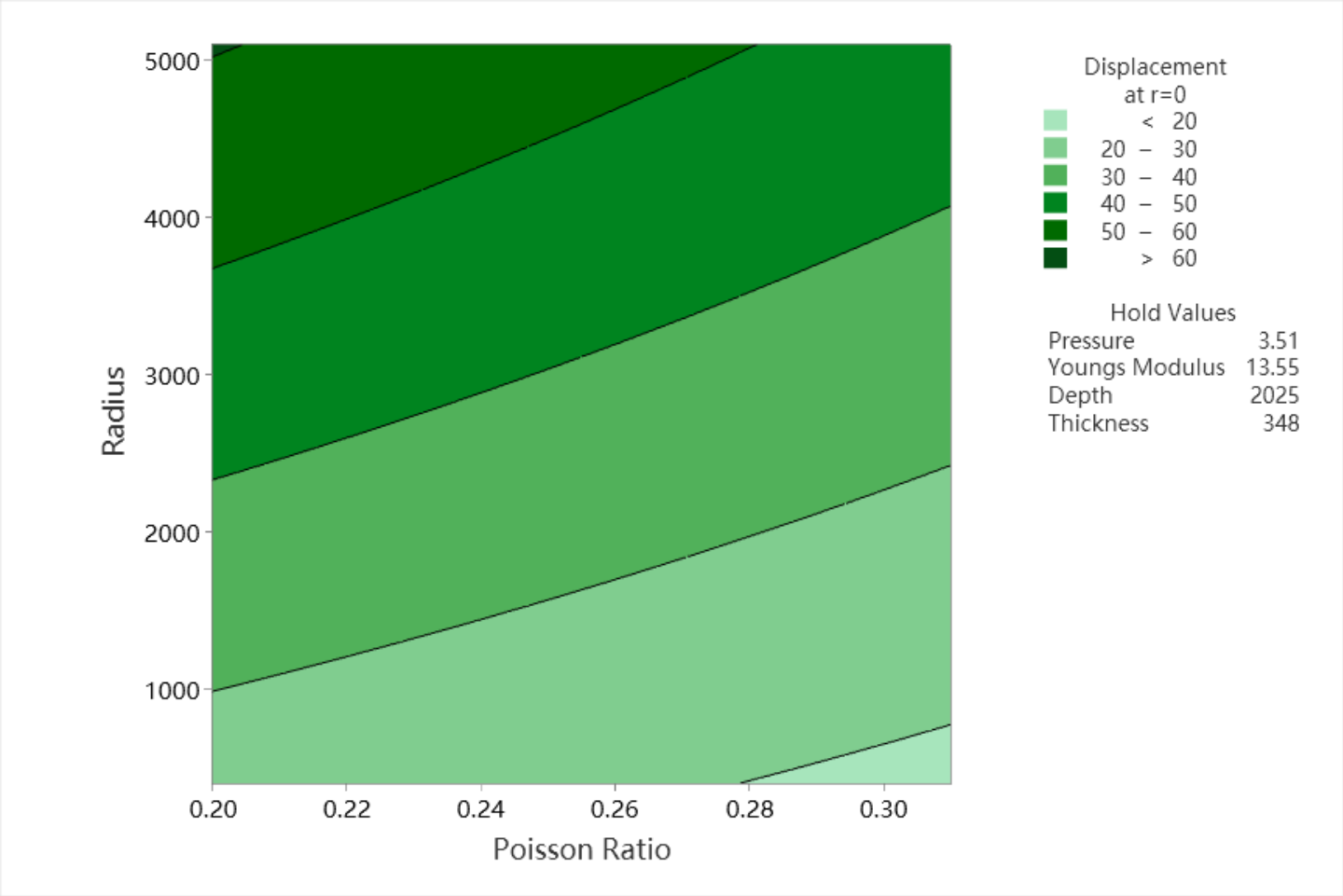

Figure 4.7: Contour Plot of Maximum Uplift vs Poisson Ratio, Radius

In contrast, the impact of Poisson's ratio, within its range (0.2–0.3), is minimal. Observing the nearly vertical contour lines, it becomes clear that changes in Poisson's ratio have negligible influence on surface uplift when the reservoir radius remains constant. This aligns with the full factorial sensitivity analysis results, confirming that Poisson's ratio has the lowest sensitivity concerning maximum surface uplift.

Poisson's ratio is the ratio between lateral deformation and longitudinal deformation, reflecting a material's deformation characteristics under stress. Its limited effect on maximum surface uplift observed in this analysis could be attributed to:

1. **Small Variation Range of Poisson's Ratio:** The relatively narrow variation range restricts the magnitude of change in longitudinal deformation, thus limiting its impact on the surface uplift.
2. **Dominant Role of Other Parameters:** Parameters such as reservoir thickness and pressure changes exert a more direct and substantial influence on surface uplift.

4.2 Sensitivity Analysis of Uplift Distribution Area

To comprehensively evaluate the sensitivity of reservoir parameter changes to surface uplift and analyze the maximum uplift value, this section further introduces the area under the curve (AUC) as an essential indicator to measure the distribution range and accumulation of surface uplift. AUC can be regarded as the integral result of the uplift profile curve above the entire injection area, reflecting the overall response of the surface deformation caused by injection on a spatial scale. Unlike the maximum uplift value, which only represents a single point extreme value, AUC is more suitable for evaluating the expansion trend of the uplift area and the changing characteristics of the total deformation energy under different parameter combinations. Based on the AUC indicator, this section will analyze each parameter's main effects and interaction effects through a full factorial experimental design to further reveal the primary control mechanism of the reservoir's physical properties and geometric characteristics on the spatial influence range of uplift.
In the Geertsma model, the surface uplift varies with radial distance. By weighted integration of the uplift curve over the entire radial range, a scalar can be obtained to measure the total surface uplift volume in the region. The calculation formula of AUC is as follows:

$$\mathrm{AUC} = \int_0^R u_z(r) \cdot 2\pi r \, dr \tag{30}$$

where $u_z(r)$ denotes the vertical uplift at radial distance r, and R is the maximum reservoir radius. This indicator overcomes the problem that the maximum value indicator is greatly affected by local anomalies to a certain extent, and can better reflect the cumulative effect of surface uplift in space.

However, it should be pointed out that AUC is essentially a volumetric total indicator and does not contain information about the distribution morphology of surface deformation. For example, two curves with different uplift ranges and peaks may have similar AUCs. Therefore, in practical analysis, AUC is more suitable as a supplement to maximum uplift rather than a substitute. Combining the two helps to evaluate the impact of parameter changes on surface response from the two dimensions of intensity and breadth.

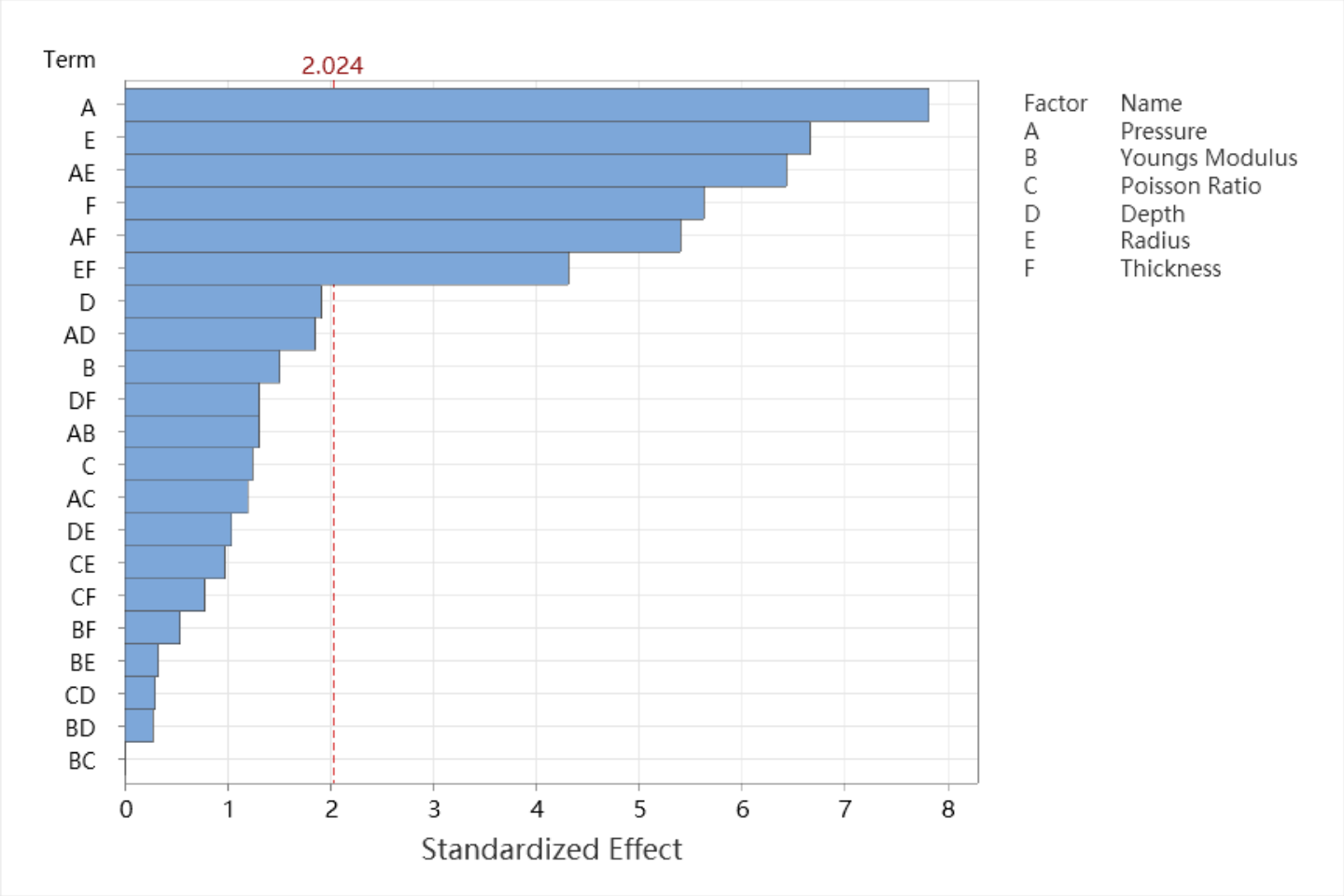

Figure 4.8: Pareto Chart of effects of model parameters on AUC

As seen from Figure 4.8, when the area under the curve is used as the response variable for sensitivity analysis, the importance of each model parameter on the result has undergone some significant changes. Pressure change is still the most important parameter affecting AUC, and its influence is significantly higher than when the maximum surface uplift is used as the response variable. This shows that pressure change determines the magnitude of surface uplift and controls the spatial distribution and total amount of the overall surface uplift to a large extent. More noteworthy is that the reservoir radius ranks second in terms of its influence on AUC, which is slightly different from the ranking in the analysis of maximum surface uplift, reflecting the important role of reservoir radius in affecting the spatial distribution and total area of surface uplift. In addition, reservoir thickness and Young's modulus also significantly impact AUC, especially since the effect of reservoir thickness is significantly higher than depth and Poisson's ratio. Poisson's ratio is a relatively small factor in the sensitivity analysis of both response variables, which means that its change has a limited impact on the magnitude and range of surface deformation.

Response Variable: Maximum Uplift	Response Variable: AUC
Pressure Change: 6.61	Pressure Change: 7.82
Thickness: 5.34	Radius: 6.67
Depth: 3.16	Thickness: 5.63
Young's Modulus: 2.96	Depth: 1.92
Radius: 2.85	Young's Modulus: 1.51
Poisson Ratio: 1.05	Poisson Ratio: 1.24

Table 4.3: Single Effect Results for Response Variables (Maximum Uplift and AUC)

According to the results given in Table 4.3, the individual effect of each parameter under different response variable conditions can be further clarified. When the response variable is the maximum surface uplift, the pressure change is still the most critical factor affecting the maximum surface uplift, followed by parameters such as thickness and depth, and Young's modulus also has a significant inhibitory effect on the maximum uplift. When the area under the curve is used as the response variable, the order of influence of each factor has changed significantly. Although the pressure change is still the most important factor, the importance of the reservoir radius has increased significantly, surpassing the thickness and becoming the second most important factor after the pressure.

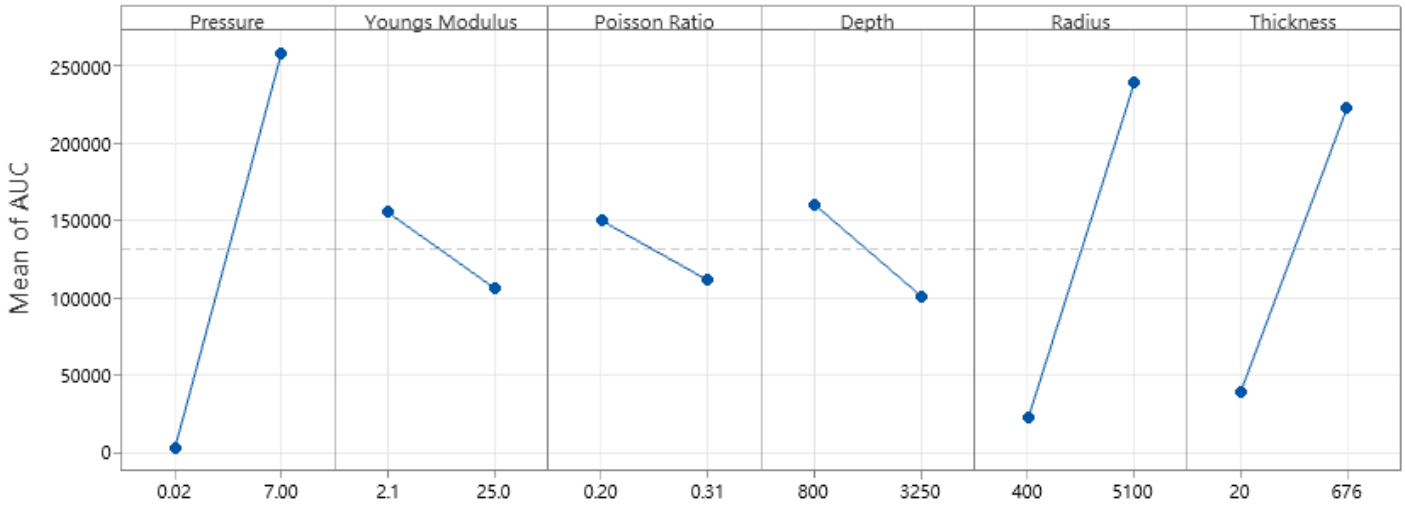

Figure 4.9: Main Effects Plot for AUC

Figure 4.9 shows the main effect responses of six geological and mechanical parameters to AUC. As can be seen from the figure, pressure change has the most significant effect on AUC. When the pressure increases from 0.02 MPa to 7.0 MPa, the AUC value rises sharply, indicating that pressure change is the primary factor controlling the overall surface uplift.

In addition to pressure change, reservoir thickness and radius also show significant positive effects, and both main effect curves are steep. This indicates that the expansion of the reservoir on vertical and horizontal geometric scales will enhance the cumulative uplift impact on the surface. Since AUC measures the total uplift within the entire radial range, it is essentially controlled by the range of the deformation area. Therefore, when the reservoir size increases, the spatial cumulative effect of surface deformation increases accordingly, which is more evident in the main effect diagram.

In contrast, the effects of Young's modulus, Poisson's ratio, and reservoir burial depth are relatively weak. Among them, Poisson's ratio has almost no impact on AUC, and the main effect curve is approximately horizontal, indicating that it contributes very little to controlling the total surface uplift. Although the response curve of Young's modulus has a certain slope, the amplitude is limited. In theory, reservoir burial depth may affect surface uplift through two mechanisms: first, the burial depth determines the initial vertical stress state; second, when the overpressure in the deep reservoir propagates upward, its energy may gradually decay during the propagation process, resulting in a weakened deformation response reaching the surface. However, under the assumption of the Geertsma model, the vertical total stress is regarded as constant, and the pore pressure propagation path is not considered. Therefore, the influence of burial depth on the calculation results is greatly simplified, and its performance on AUC is relatively insensitive.

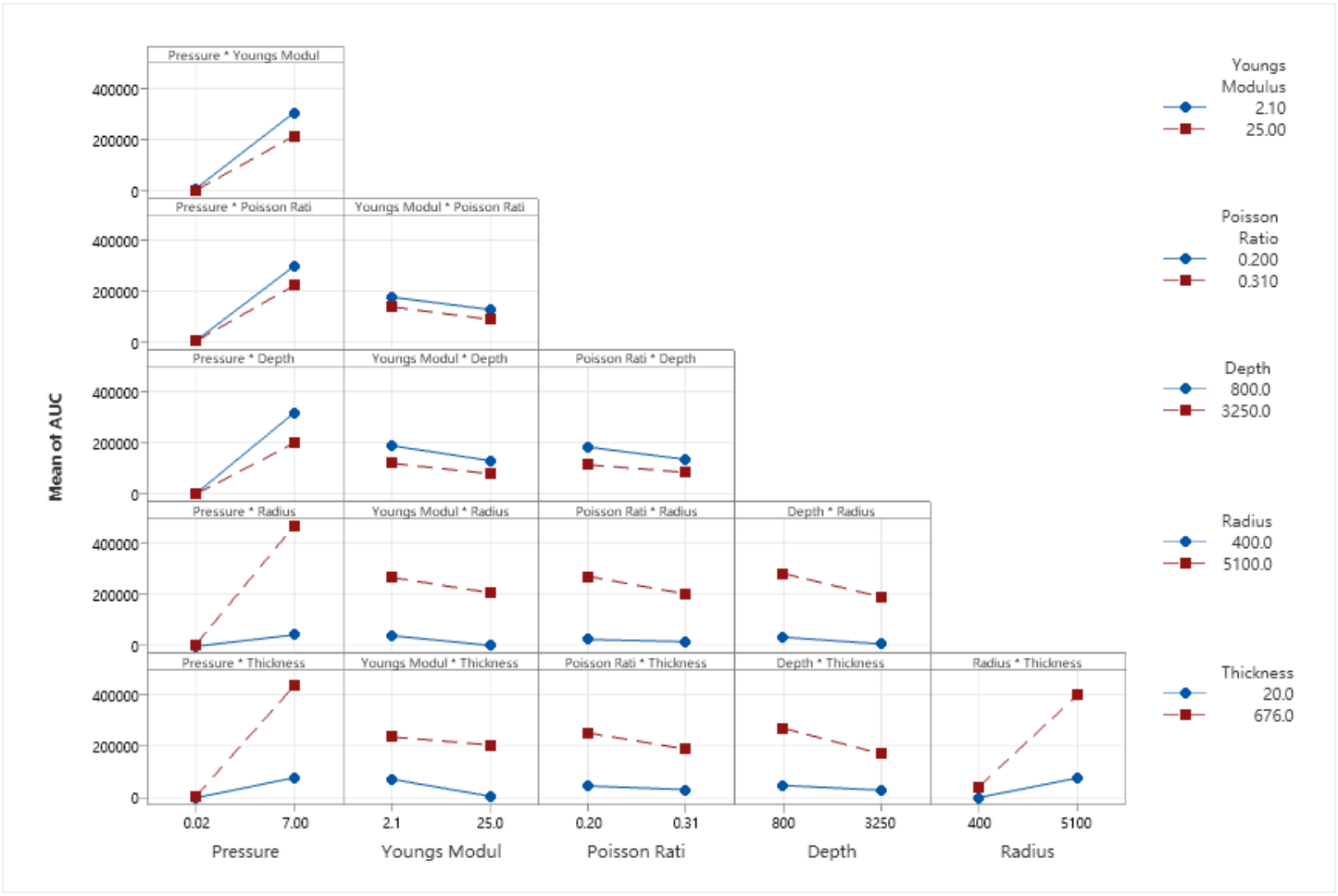

Figure 4.10: Interaction Plot for AUC

Figure 4.10 shows the interaction diagram of AUC, which is used to analyze how the combined effects of different parameters affect the spatial distribution range of surface uplift. It can be observed from the figure that one of the most influential combinations of factors is the interaction between pressure change and reservoir thickness. Under low pressure conditions, the change in reservoir thickness has no significant effect on AUC, while under high pressure scenarios, the increase in reservoir thickness significantly amplifies the area under the curve. This phenomenon shows that the effect of reservoir thickness will be amplified under high pressure change. The essential reason is that the release of formation deformation energy is more intense during high-pressure injection, and thick reservoirs provide a larger energy storage space, resulting in a wider uplift response on the surface.

In contrast, the interaction curves between other factors such as Young's modulus and Poisson's ratio are almost parallel, indicating that their combined effect on AUC is small. This may be related to the deformation mechanism of the two themselves: Young's modulus controls the overall stiffness of the rock, while Poisson's ratio mainly affects the lateral diffusion characteristics of strain. Although the two are coupled in theory, they do not show obvious synergistic effects under this model setting.

It is also worth noting that the interaction between reservoir radius and Poisson's ratio also shows a certain nonlinear relationship in the figure, especially under the condition of larger radius, the response amplitude of Poisson's ratio to AUC becomes more sensitive. This may be due to the fact that the large-scale reservoir causes the stress disturbance to propagate in the horizontal direction, so that the influence of Poisson's ratio on lateral stress transmission gradually appears.

Overall, it shows that among the control factors of AUC, the joint effect of reservoir thickness and pressure change is the most critical, while the elastic parameters themselves and their combination have relatively weak control over the total amount of uplift, which is more reflected in the local stress distribution and displacement morphology.

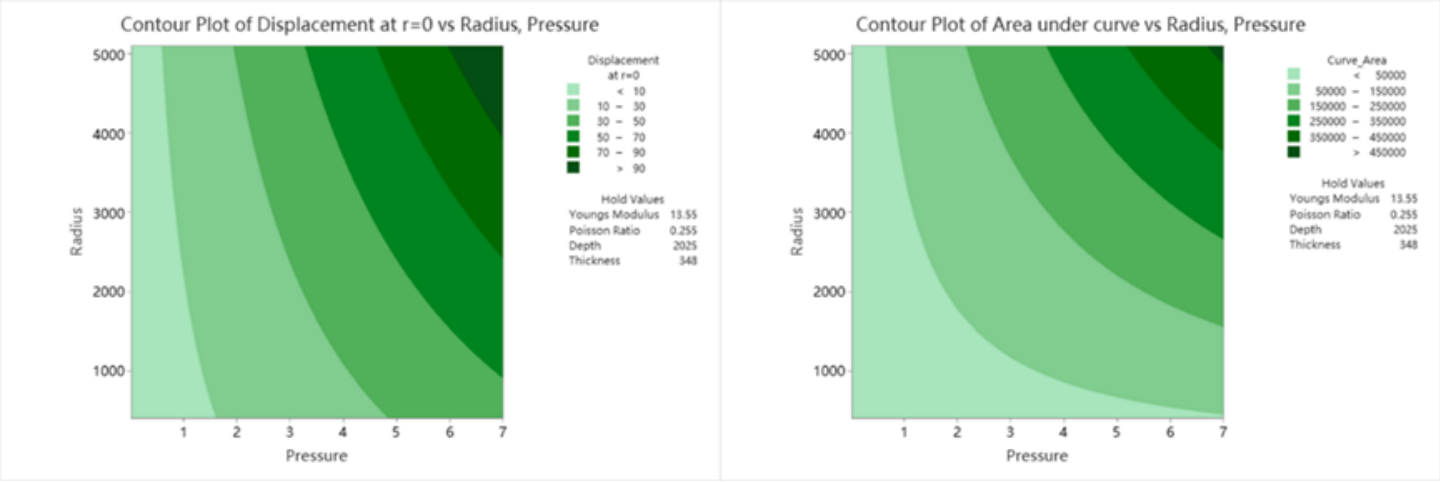

Figure 4.11: Contour Plot of Effect of Pressure Change and Radius on Maximum Uplift and AUC

Figure 4.11 is a contour map of the combined effects of pressure change and reservoir radius on maximum surface uplift and AUC. It can be clearly seen from the figure that the contour lines of maximum surface uplift are almost parallel to the pressure axis, indicating that this indicator is almost completely controlled by the pressure change and has little to do with the reservoir radius. The reason is that the maximum uplift usually occurs just above the injection point, and its formation mechanism is mainly due to local vertical stress concentration and compression release, so it is more dependent on the injection energy in the vertical direction rather than the horizontal diffusion range.

In sharp contrast to this is the distribution of AUC. The contour map of AUC shows a high sensitivity to both parameters. Under low pressure change, even if the reservoir radius is increased, it can only bring a limited uplift area; but under high pressure change, the expansion of the reservoir radius significantly increases the uplift distribution range, which in turn causes a sharp increase in AUC. The physical basis of this phenomenon is that when the pressure change increases, the stress disturbance in the reservoir can be transmitted to the surface through a wider horizontal range, and the large radius geometric characteristics make this transmission process more uniform and far-reaching, thereby promoting the expansion of the entire surface uplift area.

5 Surface Uplift Across Multiple CCS Fields

This chapter mainly analyzes the performance of the Geertsma model in predicting surface uplift at five CCS sites: In Salah, Sleipner, Weyburn, Gundih, and Saskatchewan. The surface uplift of these sites was calculated using the Geertsma model, and the calculation results were compared with the numerical simulations or satellite observation data in the existing literature. Since the Geertsma model is a simplified method based on analytical solutions, there will inevitably be some differences from the actual situation or detailed numerical simulations. This chapter will conduct a specific analysis of these differences.

During the analysis, the specific geological characteristics of each site will be combined to discuss the possible causes of the differences one by one. In addition, the sensitivity analysis results in the previous chapter will also be included in the discussion to more fully understand the impact of key parameters such as reservoir pressure changes, thickness, radius, and Poisson's ratio on the prediction results in different CCS sites. These comparative analyses reveal the applicability and limitations of the Geertsma model in practical applications more clearly.

5.1 Analysis of Surface Uplift at the In Salah Site

The surface uplift in the In Salah area is a typical case in the current CCS research field, and there are a lot of actual observation data and numerical simulation results available for verification and comparison. Therefore, this study uses the Geertsma model to calculate the surface uplift in this area and conducts an in-depth comparative analysis of the calculation results with the results obtained by the CMG numerical simulation model and satellite data to explore the differences between different models and their causes.

Table 5.1 shows the parameters required for the two models. The Geertsma model has relatively simple input parameters. The model focuses on geomechanical parameters and is relatively fast and straightforward to calculate. Therefore, it is more suitable for preliminary evaluation, rapid sensitivity analysis, and studies with limited data. CMG requires more input parameters, not only considering basic geomechanical parameters but also porosity, permeability, and detailed injection conditions.

Model-Input	**Geertsma**	**CMG-GEM**
Layer thickness [m]	Yes	Yes
Poisson's ratio	Yes	Yes
Young's modulus [GPa]	Yes	Yes
Biot coefficient	Yes	Yes
Reservoir porosity	No	Yes
Reservoir permeability [md] (Kh, Kv)	No	Yes
Rock Compressibility [1/MPa]	No	Yes
Reservoir Temperature [°C]	No	Yes
Pressure Information		
Pressure at reference depth [MPa]	No	Yes
Pressure change [MPa]	Yes	No
Injection Parameters		
Well Location	No	Yes
CO_2 injection rate [Kg/s]	No	Yes
CO_2 injection period [years]	No	Yes
Injection Pressure	No	Yes

Table 5.1: Comparison of Model Inputs Between Geertsma and CMG-GEM

Figure 5.1 shows the surface uplift in the In Salah calculated under different pressure change conditions using the Geertsma model. It can be seen intuitively from Figure 5.1a that with the increase in reservoir pressure change, the surface uplift also increases significantly, showing an apparent positive correlation; at the same time, the uplift decreases rapidly from the center to the outside, and tends to stabilize after the radial distance exceeds about 6,000 meters.

Figure 5.1b explicitly depicts the spatial distribution characteristics of the surface uplift in the In Salah caused by 5 years of CO_2 injection under the condition of 7 MPa pressure change. The figure clearly shows a circular, symmetrical uplift trend

centered on the injection area, and the maximum uplift in the central area is about 25 mm, consistent with the results of the published numerical simulation literature in order of magnitude and trend. Combined with the previous sensitivity analysis results, it can be found that pressure change is indeed the most sensitive factor causing the change in the surface uplift, which is again confirmed by the results of Figure 5.1a.

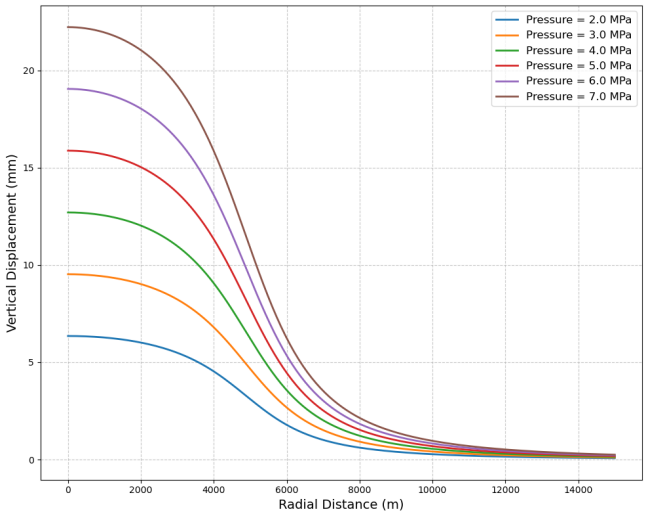

(a) Surface Displacement Profile with Different Pressure Difference

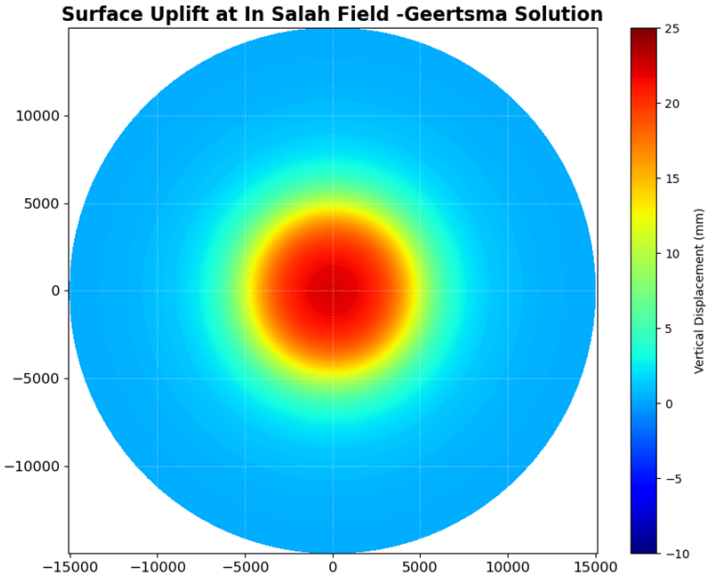

(b) Surface Uplift after Five Years of Injection

Figure 5.1: Surface Uplift for the In Salah field Calculated by Geertsma Model

Figure 1.4 shows the actual surface uplift in the In Salah observed using InSAR. It can be seen from the figure that the distribution of surface uplifts shows asymmetric characteristics. Among them, there are apparent local uplifts near the three wells of KB-501, KB-502, and KB-503, with the maximum uplift reaching about 20 mm. Compared with the uplifts predicted by the Geertsma model (Figure 5.1b), the spatial distribution of uplifts observed by satellites is more complex and does not show the ideal symmetrical circular distribution characteristics predicted by the Geertsma model. The main reasons for this difference may include reservoir heterogeneity, local geological structure differences, the complexity of CO_2 migration paths during actual injection, and the influence of regional ground stress fields, etc., and these factors are not considered by the Geertsma model.

Next, a comparative analysis is conducted between the surface uplift results obtained from the CMG numerical simulation and those calculated using the analytical Geertsma model. The modeling parameters used in CMG are shown in the Table 5.2.

CMG-GEM Model Parameters	In Salah Field
Overall model dimensions [Length×Width×Height]	20100m×20100m×2720m
Poisson's ratio	[0.20, 0.15, 0.20, 0.15]
Young's modulus [GPa]	[1.5, 20, 6, 20]
Biot coefficient	1
Porosity	0.17
Permeability [md] (Kh, Kv)	13
Reservoir Temperature [°C]	95
Pressure at reference depth [MPa]	11.8
Well Location	Center
CO_2 injection rate [Kg/s]	2459.49
CO_2 injection period [years]	5
Reference depth of injection [m]	1812

Table 5.2: CMG-GEM Model Parameters for In Salah Field

Figure 5.2 shows the reservoir model of In Salah and its surrounding geogrid model. The modeling options provided by CMG can model the reservoir and its surroundings separately. The dimensions of the reservoir are 5100m*5100m*20m, and the dimensions of the geogrid are 20100m*20100m*2720m. Since the reservoir thickness in the In Salah area is only 20 meters, the reservoir is divided into only one layer to avoid the considerable deformation caused by a small grid.

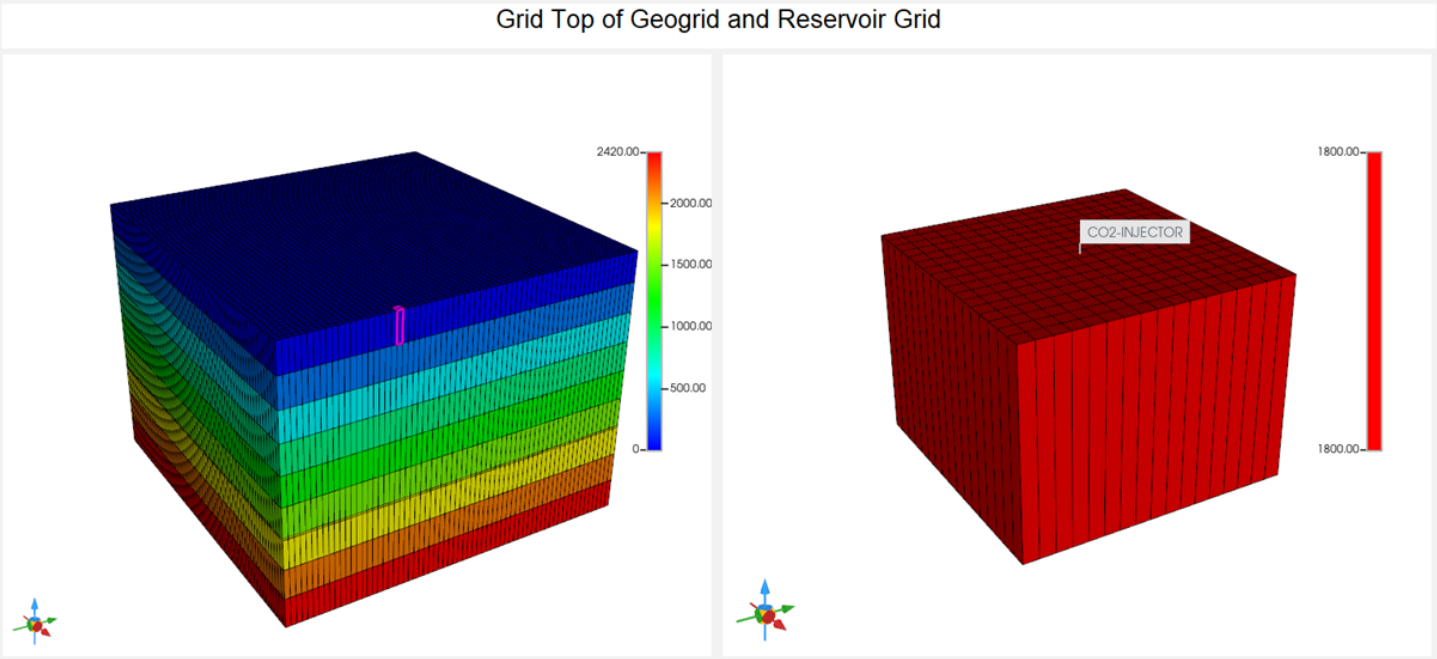

Figure 5.2: Geogrid and reservoir grid setup in CMG

The entire geogrid is divided into ten layers. Except for the reservoir, the height of other layers is 300m, and the overburden, caprock, and underburden are all set to 900m. The injection well is located at the center of the model. After simulating the injection of one million tons of carbon dioxide, the surface displacement diagram of the reservoir is shown in Figure 5.3.

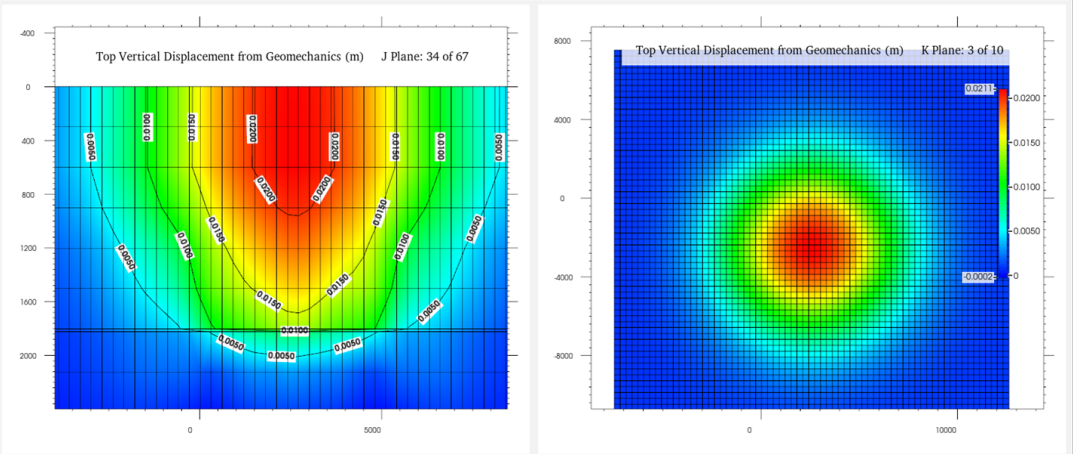

Figure 5.3: Top Vertical Displacement Results from CMG Simulation

The left figure shows the uplift of the J plane of the model, which is located in the middle of the model. The color gradient represents the magnitude of the displacement, and the red area is the maximum uplift. The contour lines show that the displacement gradually decays from the center area to the outside, and the uplift reaches the maximum value at the surface. The right figure shows the uplift distribution at the model's top (K plane). It can be seen from the figure that the displacement is radially symmetrical, with the most significant uplift in the center area (red) and gradually decreasing outward.

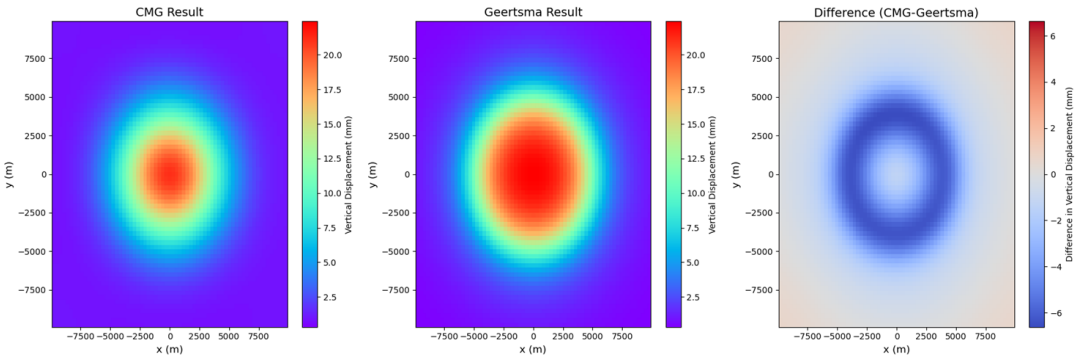

Figure 5.4: Displacement difference between Geertsma and CMG-GEM

Figure 5.4 shows the comparison results of the surface displacement predicted by the CMG-GEM numerical simulation and the Geertsma model under the same geological conditions in the In Salah area and the difference distribution map between the two. From the results calculated by the two models, the spatial distribution trend of the surface uplift is relatively consistent, both showing a symmetrical uplift centered on the injection point, and decaying rapidly with the increase of radial distance from the center point, which is also roughly consistent with the uplift distribution trend obtained by actual satellite observations.

However, from the difference distribution map, it can be found that although the CMG and Geertsma models are not much different in terms of maximum uplift values, the spatial attenuation rates of the two are significantly different, especially within a certain range from the center, the difference in surface uplift between the two can reach up to about 6 mm. Specifically, the uplift predicted by the CMG-GEM model decays faster with increasing radial distance, which may be since the CMG-GEM model takes into account the complex fluid-solid coupling effects including reservoir porosity, permeability, well location and actual injection conditions, so that it can more truly reflect the heterogeneous distribution of the pressure field under actual reservoir conditions.

The Geertsma model only considers limited geomechanical parameters during calculation, ignoring the dynamic migration of fluids and geological heterogeneity inside the reservoir. This simplification makes the predicted pressure field present an ideal uniform distribution, so the uplift distribution is relatively regular and decays slowly. At the same time, combined with the previous sensitivity analysis results, it can be seen that pressure change and reservoir thickness are the main control parameters of surface uplift, which also explains why the overall magnitude of the prediction results of the Geertsma model and the CMG model are similar under the same maximum pressure conditions, but there are obvious differences in the spatial attenuation pattern.

Compared with the InSAR data, it can be found that the actual uplift distribution is affected by actual factors such as regional stress field, reservoir heterogeneity and well setting, and is more spatially heterogeneous and asymmetric, which is closer to the results of the CMG-GEM model in trend, but there is a big difference from the ideal symmetric pattern of the Geertsma model. This difference again confirms that the Geertsma model has outstanding advantages in preliminary prediction and rapid parameter sensitivity analysis. However, when it is necessary to consider actual complex working conditions and fine quantitative analysis, its scope of application will be subject to certain limitations, and it needs to be combined with numerical simulation methods to obtain more accurate and practical prediction results.

5.2 Analysis of Surface Uplift Results for Other CCS Sites

The distribution of surface displacements caused by each CCS site is calculated by entering the data from Table 3.2 into the Geertsma model. In addition to displaying the ground displacement and radial distance relationship for each CCS site, Figure 5.5 also displays the normalized relationship.

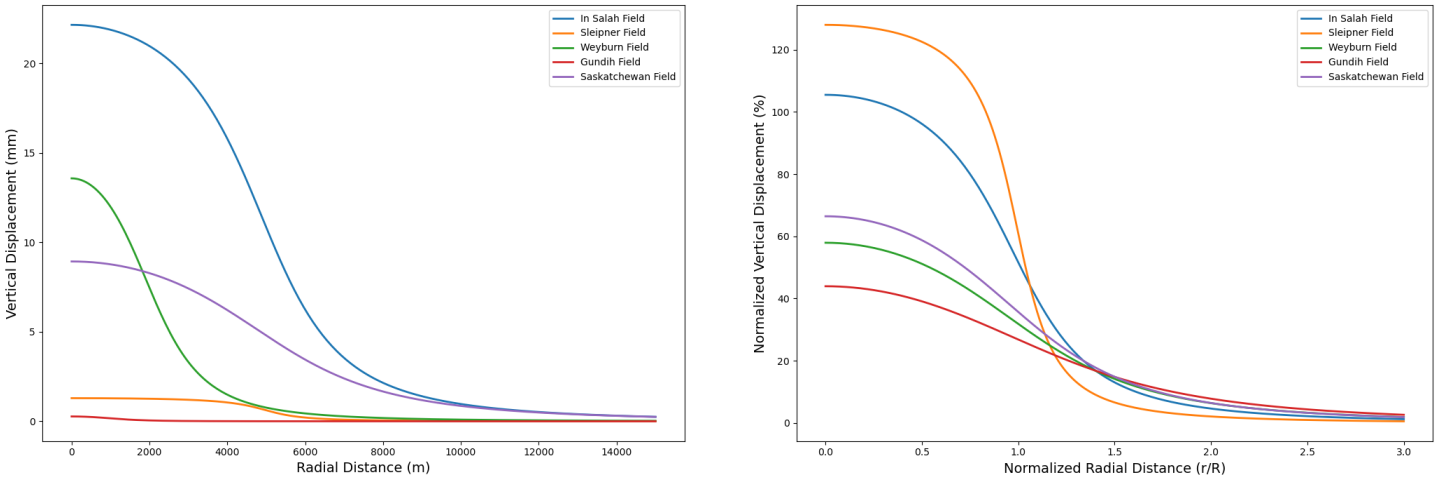

(a) Surface Displacement vs Radial Distance for Different Fields

(b) Normalized Surface Displacement vs Radial Distance

Figure 5.5: Comparison of Surface Displacement and Normalized Surface Displacement for Different Fields

According to the sensitivity analysis results, pressure change and reservoir thickness are the two most critical parameters affecting the maximum surface uplift, among which pressure change is the absolute controlling factor. This is reflected in the absolute surface uplift distribution map of each site. For example, a pressure change of 7 MPa in the In Salah area produced a significantly more significant maximum surface uplift (about 22 mm). In contrast, the maximum surface uplift in Sleipner, Weyburn, Gundih, and Saskatchewan was significantly reduced due to the relatively small pressure changes.

However, when analyzing the sensitivity of the response variable AUC in Figure 4.10, it becomes evident that the reservoir radius has a powerful influence on AUC. This is because AUC captures the vertical magnitude of surface uplift and its spatial extent. A larger reservoir radius expands the area over which uplift occurs, directly increasing the integral of vertical displacement over radial distance. As a result, even sites with modest peak uplift can yield large AUC values if their reservoir radius is sufficiently wide. Compared with the response variable of maximum surface uplift, AUC comprehensively reflects the surface uplift amplitude and spatial impact range and can, therefore, more comprehensively reveal the influence of the spatial scale parameter of reservoir radius. From the normalized surface uplift map, we can further see that even though the absolute value of the maximum surface uplift of some sites (such as Sleipner) is small (about 1.29 mm), due to the large reservoir radius (5000 m), its normalized uplift attenuation trend is significantly faster, so its AUC value may be significantly different from other sites, verifying the key role of reservoir radius in the spatial uplift distribution.

At the same time, although thickness is prominent in the sensitivity of maximum surface uplift, its significance on AUC is slightly weaker, which shows that thickness has a significant impact on the maximum uplift amplitude, but its impact on the spatial distribution of the entire uplift is slightly inferior to the reservoir radius. This can also explain why Sleipner, with a larger reservoir thickness (250 m), has a significantly different spatial distribution of uplift from other sites despite a small maximum surface uplift amplitude (about 1.29 mm).

Therefore, by considering the two response variables of maximum surface uplift and AUC simultaneously, we can more clearly understand the mechanism of the contribution of different parameters behind the uplift amplitude and spatial characteristics of each site. Specifically, high pressure changes significantly increase the amplitude of surface uplift, while the reservoir radius significantly controls the spatial impact range of the uplift. This dual-influence mechanism jointly determines the specific

surface uplift performance of each site. The Geertsma model is stable and precise in predicting the uplift trend of these sites, but it still has certain limitations in capturing the details of the complex deformation mechanism of the actual site. This chapter will analyze each site separately to explore the limitations of the Geertsma model.

5.2.1 Sleipner

Figure 5.6 illustrates the vertical displacement results at Sleipner predicted by the Geertsma model, including the radial uplift profile and the spatial distribution heatmap. The results show a peak uplift of 1.29 mm and a radially symmetric decay pattern.

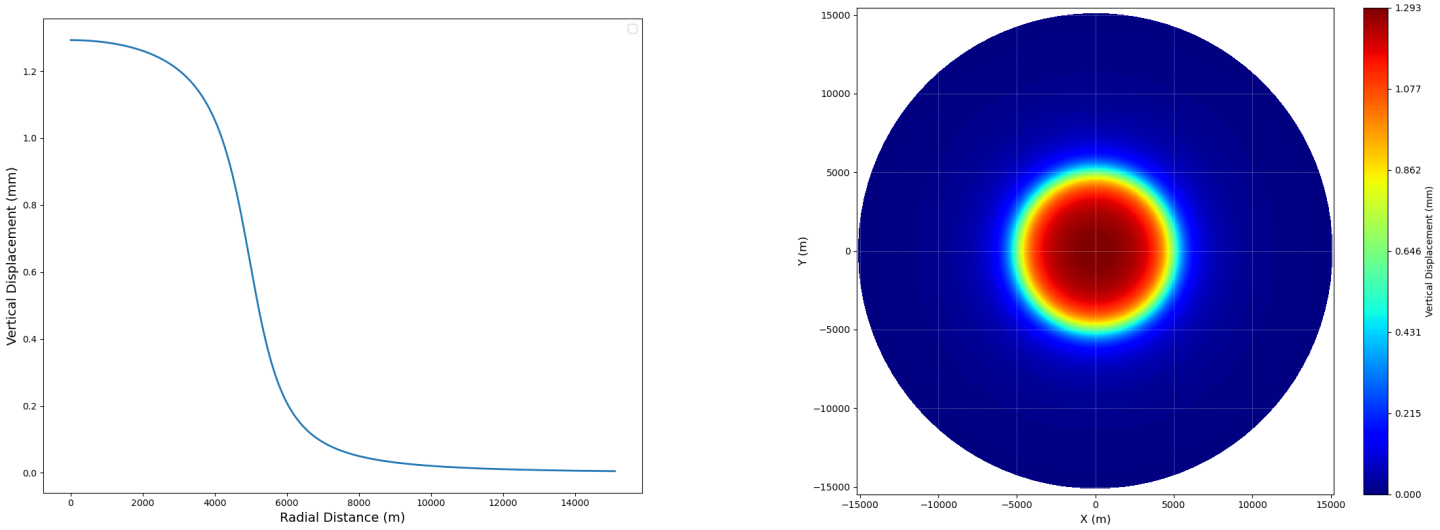

(a) Surface Uplift Profile at Sleipner

(b) Surface Uplift heatmap at Sleipner

Figure 5.6: Surface Uplift for the Slepiner field Calculated by Geertsma Model

Along with the sensitivity analysis results, it is evident that pressure change is the most significant factor influencing the amplitude of surface uplift. Even if the reservoir thickness or elastic parameters change significantly, when the pressure change is extremely small, the surface uplift still has difficulty reaching an observable scale. This conclusion is well confirmed in the Sleipner site: although the reservoir thickness is considerable (250 m) and the elastic modulus is low (2.1 GPa), which is theoretically conducive to deformation, the actual surface uplift is still very small due to the extremely low pressure change, so it has not been directly observed.

At the same time, from the perspective of the spatial distribution characteristics of the surface uplift, the Geertsma model predicts that the surface uplift of the Sleipner site decays rapidly within the reservoir radius scale, which is particularly evident in the normalized surface uplift map. Another response variable of the sensitivity analysis also shows that the reservoir radius is an important parameter affecting the spatial distribution of uplift. For the Sleipner site, a larger reservoir radius means a wider spatial influence range in theory, but due to the extremely low pressure change range of the reservoir itself, the overall surface uplift is also very limited. Therefore, the surface uplift predicted by the model is not only small overall, but the spatial attenuation characteristics are also obviously concentrated near the center, indicating that its spatial influence range is much smaller than the theoretical maximum value.

From a practical perspective, this relatively small surface uplift means that the Sleipner site has a high storage capacity, stable reservoir conditions, and good caprock integrity, which is consistent with the actual long-term operation of the project and the existing observations in the literature. Nevertheless, Chadwick and Verdon et al. (J. P. Verdon et al., 2013) still remind us that this reservoir condition is uncommon in global CCS implementation. If the storage site selected in the future does not have this ideal low pressure growth condition, it is likely to face a more significant risk of geomechanical deformation, which will pose a potential threat to storage safety.

The Geertsma model prediction results for the Sleipner site: extremely low surface uplift are consistent with the pressure changes and surface deformation expectations inferred from time-lapse seismic observations in the literature. This confirms the accuracy and applicability of the Geertsma model in low pressure change and shallow reservoir scenarios, and also verifies the importance of pressure changes in sensitivity analysis. Applying the Geertsma model at the Sleipner site generally verifies that its predictions of the surface uplift response under low-pressure change scenarios are close to actual conditions.

5.2.2 Weyburn

According to the simulation results based on the Geertsma model (5.7), the maximum surface uplift at the Weyburn site is about 13.57 mm. The uplift amplitude decays rapidly with increasing radial distance, more significant than the decay rate of surface uplift at the Slepiner site. There are currently no reports or simulation predictions on surface uplift at the site, but according to some studies, microseismic events have been observed around production wells at Weyburn (J. P. Verdon et al., 2013).

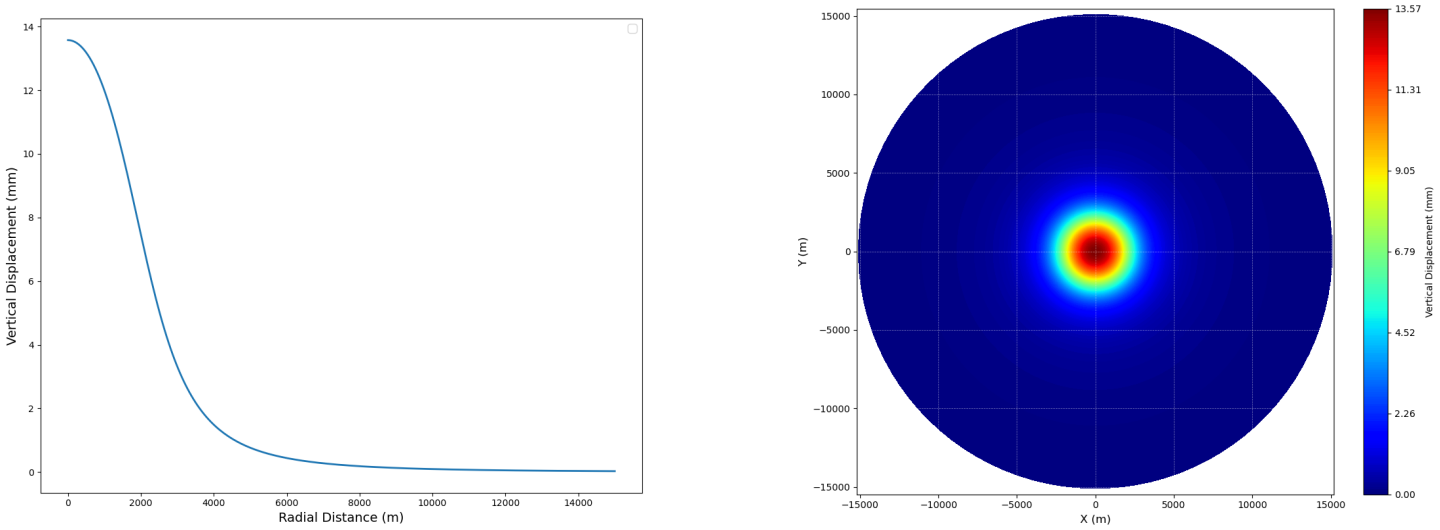

(a) Surface Uplift Profile at Weyburn

(b) Surface Uplift heatmap at Weyburn

Figure 5.7: Surface Uplift for the Weyburn field Calculated by Geertsma Model

According to the results of the sensitivity analysis, the maximum surface uplift is mainly controlled by pressure changes and reservoir thickness, which are moderate values (75 m thickness, 6.28 MPa pressure) at the Weyburn site. The high Young's modulus (14.5 GPa) limits the deformation amplitude, which leads to a relatively small surface uplift predicted by the model. The reservoir radius at the Weyburn site is 2000 m, so the surface uplift predicted by the model is concentrated and limited to the vicinity of the well area.

On the other hand, microseismic data observed in actual literature show that the stress field changes caused by reservoir deformation are not only limited to the reservoir itself but also transmitted upward to the overburden, resulting in local microseismic activity. This effect reflects that the changes in stress caused by reservoir deformation may be more extensive and complex than the range predicted by the Geertsma model. As an elastic analytical model, the Geertsma model can successfully predict the magnitude of the maximum deformation and the distribution trend of the area near the center, but it does not take into account the initial pressure history of the reservoir, the complex stress path, the fluid seepage effect, and the stress transfer phenomenon implied by the microseismic events, which explains why there is a particular deviation between the model prediction results and the actual observed phenomena on the site.

5.2.3 Gundih

According to the research of Fatkhan et al. (Suhendi et al., 2019), the surface uplift after CO_2 injection is very small and concentrated within less than 1 km around the injection well, with the maximum uplift being extremely low, less than 0.2 mm. This literature conclusion is consistent with the maximum surface uplift of about 0.27 mm calculated using the Geertsma model. The pressure change value of the Gundih site itself is extremely low (about 20,000 Pa), which directly explains the fundamental reason why it is almost impossible to observe significant macroscopic surface deformation in the area.

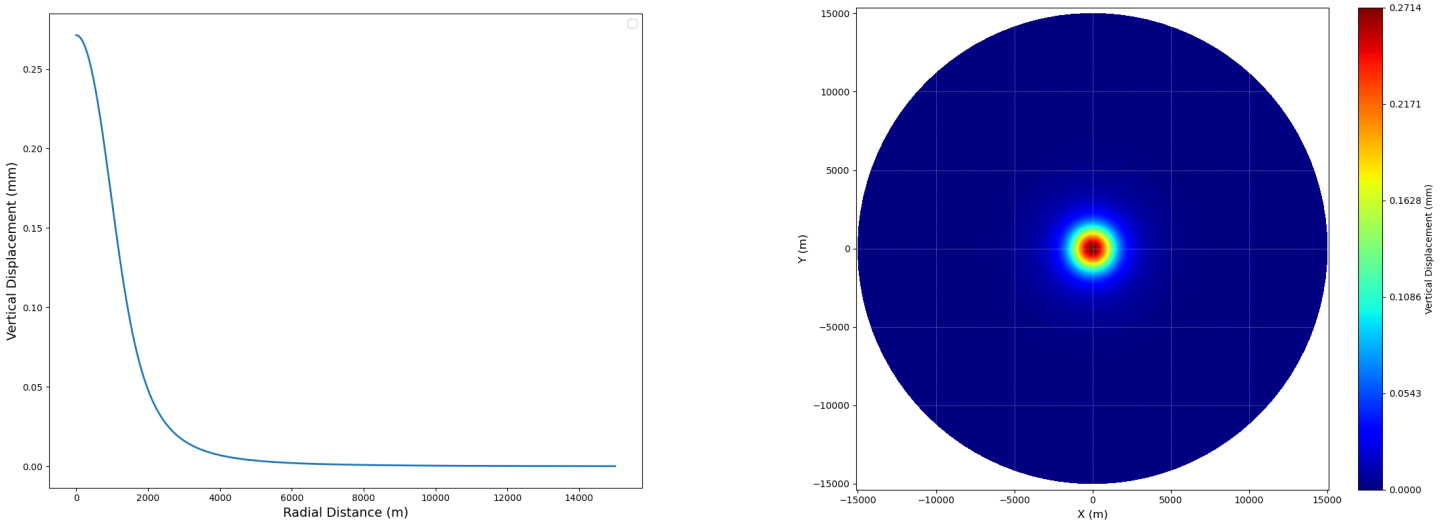

(a) Surface Uplift Profile at Gundih

(b) Surface Uplift heatmap at Gundih

Figure 5.8: Surface Uplift for the Gundih field Calculated by Geertsma Model

The prediction results of the Geertsma model (Figure 5.8) show that the surface deformation decays rapidly within a radius of 2 km. According to the sensitivity analysis results, this decay trend is caused by the extremely small radius of the reservoir (1000m). Under extremely low pressure change and extremely small radius, the overall uplift of the Gundih area is limited, so the impact area of observation is very limited. This again supports that the Geertsma model has good applicability and predictive reliability in relatively simple geological conditions, extremely small pressure changes, and stable reservoir mechanical properties.

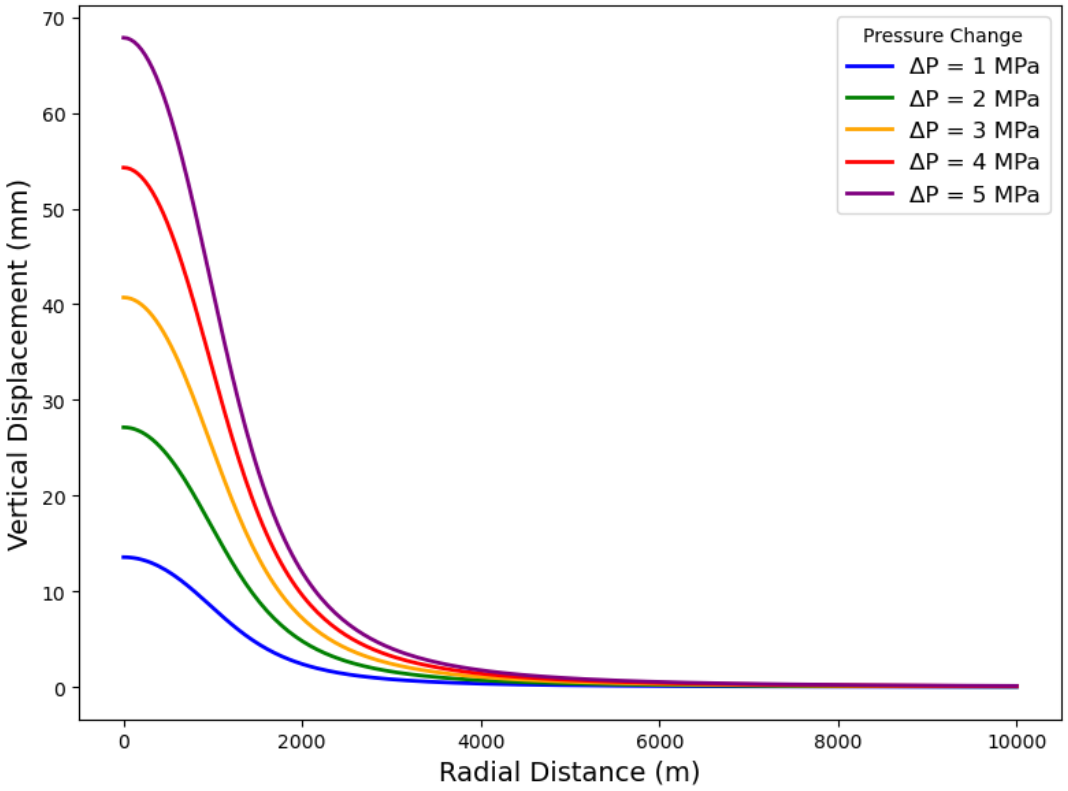

Figure 5.9: Surface uplift at Gundih with Different Pressure Change

However, in the future large-scale injection, a significant increase in reservoir pressure may bring more significant geomechanical effects. Figure 5.9 shows the surface uplift under different pressure changes. It can be seen that although the overall surface uplift is still limited by the radius, the maximum surface uplift has increased significantly. This further illustrates that even a simplified model such as the Geertsma model can accurately capture the region's basic trend and amplitude of

surface uplift, which is of great significance for the preliminary scheme evaluation. Through in-depth comparative analysis of the Gundih site, we confirmed the reliability of the Geertsma model in the scenario of small pressure changes and verified the conclusion proposed in the previous sensitivity analysis, that is, pressure changes have a decisive effect on the absolute value of surface uplift, and the influence of reservoir radius and elastic parameters on the spatial distribution characteristics of surface uplift is reflected in both literature and model results.

5.2.4 Saskatchewan

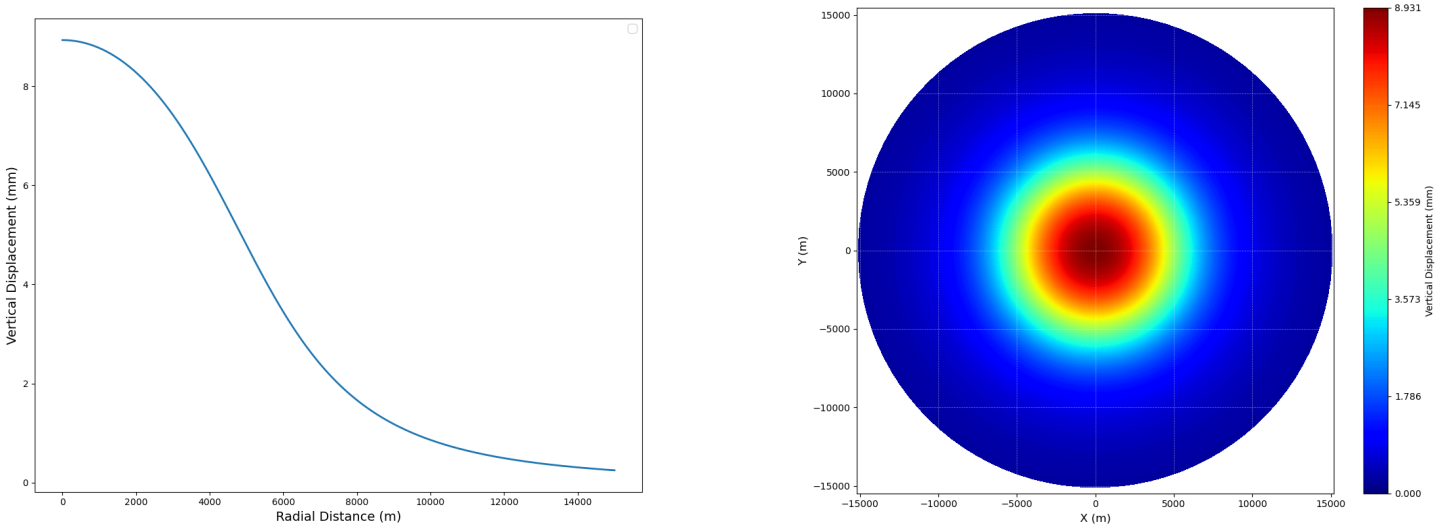

(a) Surface Uplift Profile at Saskatchewan

(b) Surface Uplift heatmap at Saskatchewan

Figure 5.10: Surface Uplift for the Saskatchewan field Calculated by Geertsma Model

According to the calculation results of the Geertsma model 5.10, assuming that the reservoir pressure change at the Saskatchewan site is 7 MPa, the maximum uplift of the surface center is about 8.93 mm. This value is significantly smaller than the previous In Salah area, but it is still much larger than the previous sites with smaller pressure changes. This result is mainly related to the higher Young's modulus (25 GPa) and larger reservoir depth (3250 m) of the Saskatchewan site. The combined effect of these two parameters suppresses the deformation response caused by reservoir pressure changes.

Young's modulus plays a key role in limiting the overall deformation amplitude. Although the pressure change at the Saskatchewan site is also significant in this hypothetical situation, the larger reservoir depth (3250 m) and higher Young's modulus (25 GPa) limit its deformation. The numerical simulation results in the literature (Samsonov et al., 2015) indicate that the surface deformation predicted by actual observations or numerical simulations is also very limited, with the maximum deformation not exceeding 16 mm. The maximum uplift predicted by the Geertsma model is about 8.93 mm, which is lower than the possible upper limit given in the literature, but the magnitude is consistent.

At the same time, from the results of normalized surface uplift, the spatial attenuation pattern of the Saskatchewan site is similar to that of other sites, showing a trend of maximum center and outward attenuation, but compared with the Sleipner site, the spatial attenuation trend is relatively mild. This is mainly because the Saskatchewan site has a larger reservoir radius and a larger reservoir burial depth, which makes the surface uplift relatively wider, which is consistent with the key influence of the reservoir radius on the spatial distribution of deformation emphasized in the sensitivity analysis conclusion of the area under the curve.

5.3 Summary of Geertsma Model Performance

This chapter evaluates the surface uplift prediction effect of the classic Geertsma model on five typical CCS sites: Salah, Sleipner, Weyburn, Gundih, and Saskatchewan. A detailed comparative analysis and discussion are conducted by combining sensitivity analysis, existing literature data, actual field observation data and numerical simulation results.

The sensitivity analysis results show that reservoir pressure change and thickness are the two most significant factors affecting the maximum surface uplift, which has been fully confirmed in the actual site analysis. For example, the In Salah site has a significantly higher surface uplift than other sites due to its significantly larger pressure change and appropriate reservoir thickness (20 m), while the Sleipner site has a larger thickness (250 m), but its surface uplift is significantly smaller due to the

extremely limited actual reservoir pressure change. Similarly, the predicted surface uplift values at the Weyburn, Gundih, and Saskatchewan sites also show good correspondence with the pressure conditions, thickness, and elastic parameters, reflecting the reliability of the Geertsma model in capturing the effects of these parameters on surface uplift.

In addition, by further analyzing the sensitivity analysis results with the area under the curve as the response variable, it was found that the reservoir radius has a significant impact on the spatial distribution range of surface uplift, while the reservoir depth and Young's modulus have an inhibitory effect on the overall deformation amplitude and spatial concentration. This conclusion was further verified in the specific analysis of the five sites. For example, although the absolute uplift amplitude of the Sleipner site is small, the spatial uplift distribution is concentrated and decays rapidly, while the surface deformation amplitude of the Saskatchewan site with a large reservoir depth and high elastic modulus is also significantly limited, which is highly consistent with the conclusions of the sensitivity analysis.

CCS Site	**Maximum Uplift (Literature) [mm]**	**Geertsma Model Prediction [mm]**
In Salah Field	25 (J. Rutqvist et al., 2011)	23.17
Sleipner Field	No significant surface deformation (J. P. Verdon et al., 2013)	1.29
Weyburn Field	No reported uplift	13.57
Gundih Field	0.2 (short-term simulation)(Suhendi et al., 2019)	0.27
Saskatchewan Field	16 (Samsonov et al., 2015)	8.93

Table 5.3: Comparison of Maximum Surface Uplift from Literature and Geertsma Model

In the comparative analysis with existing literature and actual monitoring data (Table 5.3), we also clearly found that the Geertsma model shows a high degree of prediction accuracy under low pressure change conditions (such as Sleipner and Gundih fields), which is highly consistent with the actual monitoring or literature numerical simulation results. However, when the actual site involves more complex physical mechanisms, such as the microseismic events induced by stress transfer observed in the Weyburn area, the Geertsma model can be used to predict the ground's surface. These complex factors cannot be effectively reflected under the simple elastic half-space assumption of the Geertsma model, resulting in a certain gap between the model results and the actual site.

Overall, the Geertsma analytical model can play an important role in the preliminary site assessment, rapid parameter sensitivity analysis, and early project decision-making stages due to its simplicity, computational efficiency, and clear theoretical physics basis, especially in scenarios with limited data. The prediction performance is particularly good. However, due to the simplified assumptions, the Geertsma model cannot fully cover the actual deformation process under all complex site conditions. Therefore, when facing specific engineering projects, it is recommended to further combine long-term on-site monitoring data, advanced numerical simulation, and microseismic monitoring to ensure a more comprehensive and accurate evaluation and prediction. This comprehensive analysis method can effectively reduce the uncertainty of the prediction, thereby providing a more solid and reliable basis for the safety assessment and long-term stable operation of the CCS project.

6 Conclusion

This study focuses on the applicability and accuracy of the Geertsma model in predicting the surface uplift effect during CCS, aiming to evaluate its performance characteristics under different geological conditions and clarify the influence mechanism of the model's input parameters on the prediction results through sensitivity analysis. By constructing a two-dimensional axisymmetric analytical model, conducting a full factorial experimental design and simulating and comparing five actual CCS sites, the model's capabilities and limitations in deformation prediction were systematically evaluated.

The sensitivity analysis shows that reservoir pressure change is the primary factor controlling the maximum surface uplift amplitude, and its contribution is much higher than that of other parameters. The influence of reservoir thickness and radius is second, mainly determining the spatial scale and cumulative volume of the uplift. Although the elastic modulus and burial depth affect the amplitude adjustment to a certain extent, their relative role is small; Poisson's ratio has the weakest influence among all parameters and can almost be regarded as a secondary factor. In addition, by introducing the AUC as the second response, the maximum uplift value is effectively supplemented in the spatial scale characterization, especially in evaluating the reservoir influence range and the remote deformation attenuation characteristics.

In the analysis of the simulation results of five typical CCS sites, it was found that the Geertsma model has good prediction consistency in sites with a single geological structure and a clear injection range. For example, in sites such as In Salah and Gundih, the uplift trend predicted by the model is consistent with the CMG numerical simulation results, indicating that its simulation of elastic response under homogeneous medium conditions is credible. In the Sleipner site, due to the extremely low pressure change, the model predicts a smaller maximum uplift value despite the large reservoir thickness, indicating that the model can reasonably reflect the deformation in a low-pressure change scenario.

However, in complex sites such as Weyburn, there is a large deviation between the model and the actual monitoring results. The main reason is that there are obvious lithological heterogeneity, fracture development and stress redistribution in the Weyburn reservoir, and the Geertsma model itself is based on the assumptions of isotropy, linear elasticity and homogeneous medium, and fails to capture these factors that have a key impact on the deformation mode in the actual geological environment. This comparison shows that although the model can be used for trend assessment, its application results must be interpreted cautiously under the conditions of multi-layer, heterogeneous, or fracture-controlled reservoirs. It is recommended to combine field monitoring or numerical simulation for multi-method cross-validation.

The results of this study provide a concise and effective analysis tool for early site selection assessment and surface uplift risk screening of CCS sites. In the case of limited data or computing resources, the Geertsma model can be used as a fast estimation scheme for preliminary identification of high-risk areas or comparative evaluation between multiple sites. Its prediction results have high engineering practical value, especially in sites with known pressure evolution and relatively uniform lithology.

Future research can be further explored in the following aspects: First, construct a hybrid modeling framework that couples analytical models with numerical simulation methods (such as CMG-GEM, FLAC3D, etc.) to balance accuracy and efficiency; second, combine remote sensing monitoring methods (such as InSAR time series interferometry) to verify model predictions in the field to improve the reliability of its parameter calibration and spatial deformation response; third, introduce nonlinear material models and heterogeneous structural parameters to gradually enhance the adaptability of analytical models to complex actual sites and expand their application scope in the long-term storage stability assessment of CCS.

In summary, the Geertsma model, as a classic analytical tool, can effectively predict the surface deformation characteristics caused by CCS under specific conditions; at the same time, we should also face up to its applicable boundaries and theoretical simplifications, and give full play to its advantages of efficient calculation and clear structure in the complementary use with numerical methods and measured data, to provide support for CCS site selection, monitoring and risk assessment.

References

Abidoye, L. K., Khudaida, K. J., & Das, D. B. (2015). Geological carbon sequestration in the context of two-phase flow in porous media: a review. *Critical Reviews in Environmental Science and Technology*, *45*(11), 1105–1147.

Aminu, M. D., Nabavi, S. A., Rochelle, C. A., & Manovic, V. (2017). A review of developments in carbon dioxide storage. *Applied Energy*, *208*, 1389–1419.

Asikin, A., Sule, R., Priyono, A., Tsuji, T., & Raharjo, S. (2015). Simulation of time lapse seismic for CO_2-injection monitoring: preliminary result. In *Proceedings of the 12th segj international symposium, tokyo, japan, 18-20 november 2015* (pp. 106–109).

Asikin, A. R., Priyono, A., Ariadji, T., Sapiie, B., Sule, M. R., Tsuji, T., ... Rahardjo, S. (2018). Forward modeling time-lapse seismic based on reservoir simulation result on the ccs project at gundih field, indonesia. *Modern Applied Science*, *12*(1), 1–75.

Audigane, P., Gaus, I., Czernichowski-Lauriol, I., Pruess, K., & Xu, T. (2007). Two-dimensional reactive transport modeling of CO_2 injection in a saline aquifer at the sleipner site, north sea. *American journal of science*, *307*, 974–1008.

Baklid, A., Korbol, R., & Owren, G. (1996). Sleipner vest CO_2 disposal, CO_2 injection into a shallow underground aquifer. In *Spe annual technical conference and exhibition?* (pp. SPE–36600).

Budinis, S., Krevor, S., Mac Dowell, N., Brandon, N., & Hawkes, A. (2018). An assessment of ccs costs, barriers and potential. *Energy strategy reviews*, *22*, 61–81.

Chadwick, R., Williams, G., Williams, J., & Noy, D. (2012). Measuring pressure performance of a large saline aquifer during industrial-scale CO_2 injection: The utsira sand, norwegian north sea. *International Journal of Greenhouse Gas Control*, *10*, 374–388.

Class, H., Ebigbo, A., Helmig, R., Dahle, H. K., Nordbotten, J. M., Celia, M. A., ... Fan, Y. (2009). A benchmark study on problems related to CO_2 storage in geologic formations: summary and discussion of the results. *Computational geosciences*, *13*, 409–434.

da Fontoura, S. A. B. (2016). *Desenvolvimento e aplicação de um esquema de acoplamento termo-hidro-mecânico-químico iterativo visando o armazenamento geológico de CO_2* (Unpublished doctoral dissertation). PUC-Rio.

Enyi, Y., Yuan, D., Hui, W., Xiaopeng, C., Qingfu, Z., & Chuanbao, Z. (2023). Numerical simulation on risk analysis of CO_2 geological storage under multi-field coupling: A review. *Chinese Journal of Theoretical and Applied Mechanics*, *55*(9), 2075–2090.

Espinoza, D. N., & Santamarina, J. C. (2017). CO_2 breakthrough—caprock sealing efficiency and integrity for carbon geological storage. *International Journal of Greenhouse Gas Control*, *66*, 218–229.

Falkowski, P., Scholes, R. J., Boyle, E., Canadell, J., Canfield, D., Elser, J., ... others (2000). The global carbon cycle: a test of our knowledge of earth as a system. *science*, *290*(5490), 291–296.

Fjaer, E. (2008). *Petroleum related rock mechanics* (Vol. 491). Elsevier.

Frangeul, J., Nghiem, L., Caroli, E., & Thibeau, S. (2004). Sleipner/utsira CO_2 geological storage: full field flow and geochemical coupling to assess the long term fate of the CO_2. *AAPG Bulletin*, *88*(13).

Galloway, D. L., & Hoffmann, J. (2007). The application of satellite differential sar interferometry-derived ground displacements in hydrogeology. *Hydrogeology Journal*, *15*, 133–154.

Geertsma, J. (1973). Land subsidence above compacting oil and gas reservoirs. *Journal of petroleum technology*, *25*(06), 734–744.

Helm, D. C. (1978). Field verification of a one-dimensional mathematical model for transient compaction and expansion of a confined aquifer system.

International Energy Agency. (2023). *CO_2 emissions in 2023: Emissions grew in 2023 but clean energy is limiting the growth.* Retrieved from `https://www.iea.org/reports/co2-emissions-in-2023/emissions-grew-in-2023-but-clean-energy-is-limiting-the-growth` (Accessed: 2024-12-05)

Islam, M. N., & Pramanik, A. (2016). Comparison of design of experiments via traditional and taguchi method. *Journal of Advanced Manufacturing Systems*, *15*(03), 151–160.

Jafari, A., Talman, S., & Perkins, E. (2011). Numerical simulation of four-pattern CO_2-flood eor in the weyburn phase 1b area. *Alberta Innovates Technology Futures (AITF), Edmonton, Canada*.

Jeffry, L., Ong, M. Y., Nomanbhay, S., Mofijur, M., Mubashir, M., & Show, P. L. (2021). Greenhouse gases utilization: A review. *Fuel*, *301*, 121017.

Jiang, X. (2011). A review of physical modelling and numerical simulation of long-term geological storage of CO_2. *Applied energy*, *88*(11), 3557–3566.

Jun, S., Song, Y., Wang, J., & Weijermars, R. (2023). Formation uplift analysis during geological co2-storage using the gaussian pressure transient method: Krechba (algeria) validation and south korean case studies. *Geoenergy Science and Engineering*, *221*, 211404.

Khan, S., Khulief, Y., Al-Shuhail, A., Bashmal, S., & Iqbal, N. (2020). The geomechanical and fault activation modeling during CO_2 injection into deep minjur reservoir, eastern saudi arabia. *Sustainability*, *12*(23), 9800.

Khazaei, C., & Chalaturnyk, R. (2017). A reservoir–geomechanical model to study the likelihood of tensile and shear failure in the caprock of weyburn ccs project with regard to interpretation of microseismic data. *Geotechnical and Geological Engineering*, *35*(6), 2571–2595.

Kolivand, F., & Rahmannejad, R. (2018). Estimation of geotechnical parameters using taguchi's design of experiment (doe) and back analysis methods based on field measurement data: Case study: Tehran metro line no. 7. *Bulletin of Engineering Geology and the Environment*, *77*, 1763–1779.

Li. (2016). The geomechanics of shenhua carbon dioxide capture and storage (ccs) demonstration project in ordos basin, china. *Journal of Rock Mechanics and Geotechnical Engineering*, *8*(6), 948–966.

Mehrabian, A., & Abousleiman, Y. N. (2015). Geertsma's subsidence solution extended to layered stratigraphy. *Journal of Petroleum Science and Engineering*, *130*, 68–76.

Metz, B., Davidson, O., De Coninck, H., Loos, M., & Meyer, L. (2005). *Ipcc special report on carbon dioxide capture and storage*. Cambridge: Cambridge University Press.

Mindlin, R. D., & Cheng, D. H. (1950a). Nuclei of strain in the semi-infinite solid. *Journal of Applied Physics*, *21*(9), 926–930.

Mindlin, R. D., & Cheng, D. H. (1950b). Thermoelastic stress in the semi-infinite solid. *Journal of Applied Physics*, *21*(9), 931–933.

Mogi, K. (1958). Relations between the eruptions of various volcanoes and the deformation of the ground surfaces. *WAU-THIER ET AL*, *64*.

Morita, N. (2022). *Geomechanics of sand production and sand control*. Gulf Professional Publishing.

Park, J., Bjørnarå, T. I., & Bohloli, B. (2021). An analytical solution for pressure-induced deformation of anisotropic multilayered subsurface. *Geosciences*, *11*(4), 180.

Park, J., Eiken, O., Bjørnarå, T. I., & Bohloli, B. (2021). Generalized geertsma solution for isotropic layered medium. In *Tccs–11. co2 capture, transport and storage. trondheim 22nd–23rd june 2021 short papers from the 11th international trondheim ccs conference.*

Pradhan, R. P., Nair, M. S., Hall, J. H., & Bennett, S. E. (2024). Planetary health issues in the developing world: Dynamics between transportation systems, sustainable economic development, and co2 emissions. *Journal of Cleaner Production*, *449*, 140842.

Preisig, M., & Prévost, J. H. (2011). Coupled multi-phase thermo-poromechanical effects. case study: CO_2 injection at in salah, algeria. *International Journal of Greenhouse Gas Control*, *5*(4), 1055–1064.

Russell, K. G. (2018). *Design of experiments for generalized linear models*. Chapman and Hall/CRC.

Rutqvist, & Tsang. (2002). A study of caprock hydromechanical changes associated with CO_2-injection into a brine formation. *Environmental Geology*, *42*, 296–305.

Rutqvist, J., Liu, H.-H., Vasco, D. W., Pan, L., Kappler, K., & Majer, E. (2011). Coupled non-isothermal, multiphase fluid flow, and geomechanical modeling of ground surface deformations and potential for induced micro-seismicity at the in salah co2 storage operation. *Energy Procedia*, *4*, 3542–3549.

Rutqvist, J., Vasco, D. W., & Myer, L. (2010). Coupled reservoir-geomechanical analysis of co2 injection and ground deformations at in salah, algeria. *International Journal of Greenhouse Gas Control*, *4*(2), 225–230.

Rutqvist, J., Wu, Y.-S., Tsang, C.-F., & Bodvarsson, G. (2002). A modeling approach for analysis of coupled multiphase fluid flow, heat transfer, and deformation in fractured porous rock. *International Journal of Rock Mechanics and Mining Sciences*, *39*(4), 429–442.

Rychlewski, J. (1984). On hooke's law. *Journal of Applied Mathematics and Mechanics*, *48*(3), 303–314.

Samsonov, S., Czarnogorska, M., & White, D. (2015). Satellite interferometry for high-precision detection of ground deformation at a carbon dioxide storage site. *International Journal of Greenhouse Gas Control*, *42*, 188–199.

Sen, B. (1951). Note on the stresses produced by nuclei of thermo-elastic strain in a semi-infinite elastic solid. *Quarterly of Applied Mathematics*, *8*(4), 365–369.

Song, J., & Zhang, D. (2013). Comprehensive review of caprock-sealing mechanisms for geologic carbon sequestration. *Environmental science & technology*, *47*(1), 9–22.

Suhendi, C., Sahara, D. P., & Sule, M. R. (2019). Modeling geomechanical responses induced by CO_2 injection in ccs pilot project in gundih field, indonesia. In *Journal of physics: Conference series* (Vol. 1204, p. 012106).

Sule, R., Kadir, W. G. A., Hato, M., Matsuoka, T., & Prabowo, H. (n.d.). Gundih ccs: The first carbon capture and storage project in south and southeast asia regions.

Teatini, P., Gambolati, G., Ferronato, M., Settari, A. T., & Walters, D. (2011). Land uplift due to subsurface fluid injection. *Journal of Geodynamics*, *51*(1), 1–16.

Varanda, C., Portugal, I., Ribeiro, J., Silva, A. M., & Silva, C. M. (2017). Optimization of bitumen formulations using mixture design of experiments (mdoe). *Construction and Building Materials*, *156*, 611–620.

Verdon, J. (2011). Microseismic monitoring and geomechanical modeling of CO_2 storage in subsurface reservoirs. *Geophysics*, *76*(5), Z102–Z103.

Verdon, J. P., Kendall, J.-M., Stork, A. L., Chadwick, R. A., White, D. J., & Bissell, R. C. (2013). Comparison of geomechanical deformation induced by megatonne-scale co2 storage at sleipner, weyburn, and in salah. *Proceedings of the National Academy of Sciences*, *110*(30), E2762–E2771.

Verseput, R. (2000). *Digging into doe: Selecting the right central composite design for response surface methodology applications. quality digest.*

Weijermars, R. (2023). Surface subsidence and uplift resulting from well interventions modeled with coupled analytical solutions: Application to groningen gas extraction (netherlands) and CO_2-eor in the kelly-snyder oil field (west texas). *Geoenergy Science and Engineering*, *228*, 211959.

White, J. A., Chiaramonte, L., Ezzedine, S., Foxall, W., Hao, Y., Ramirez, A., & McNab, W. (2014). Geomechanical behavior of the reservoir and caprock system at the in salah CO_2 storage project. *Proceedings of the National Academy of Sciences*, *111*(24), 8747–8752.

Wikipedia. (2025, February 6). *Full factorial experiment.* Retrieved from `https://en.wikipedia.org/wiki/Full_factorial_experiment` ([Online; accessed 12-February-2025])

Xiao. (2016). A review of numerical simulation methods for geomechanical problems induced by CO_2 geological storage. *Rock and Soil Mechanics*, *37*(6), 1762–1772.

Yin, S., Dusseault, M. B., & Rothenburg, L. (2011). Coupled thmc modeling of CO_2 injection by finite element methods. *Journal of Petroleum Science and Engineering*, *80*(1), 53–60.

Zhang, Y., Hao, S., Yu, Z., Li, X., & Xu, T. (2018). Land uplift induced by injection: a feasible method to evaluate the security of co 2 capture and sequestration projects. *Environmental Earth Sciences*, *77*, 1–11.

Zweigel, P., Arts, R., Lothe, A. E., & Lindeberg, E. B. (2004). Reservoir geology of the utsira formation at the first industrial-scale underground CO_2 storage site (sleipner area, north sea). *Geological Society, London, Special Publications*, *233*(1), 165–180.